PRELIMINARY INDIAN OCEAN SWORDFISH STOCK ASSESSMENT 1950-2018 (STOCK SYNTHESIS)

PREPARED BY: DAN FU[1],

02 AUGUST 2020

---

[1] IOTC Secretariat, Dan.Fu@fao.org;

Contents

SUMMARY

This report presents a preliminary stock assessment for Indian Ocean swordfish (*Xiphias gladius*) using *Stock Synthesis 3* (SS3). The assessment uses a spatially disaggregated, sex explicit, and age structured model that integrates several sources of fisheries and biological data. The assessment model covers the period 1950–2018 and represents an update and revision of the 2017 assessment model with the inclusion of updated longline CPUE indices, and a revised fleet structure. A range of sensitivity models are also presented to explore the impact of key data sets and model assumptions.

The assessment assumed the Indian Ocean swordfish constitute a single spawning stock partitioned into 4 spatial areas (NW, NE, SW, and SE), to account for differential abundance and depletion levels among regions. The assessment model defined 15 fisheries, based on fleet and region. Standardised CPUE series (as relative abundance indices) are available from the Japanese, Taiwanese，Portuguese, Spanish, South African, and Indonesia longline fleets. The final model options focused pm the Japanese (for 4 regions), Portuguese (SW), and South African (SW) indices, assuming that they are proportional to the regional abundance of swordfish. The utility of CPUE indices from other fleets were assessed in sensitivity models. Length compositions data are available for 14 fisheries. Separate selectivities were estimated for each fleet but were assumed to be common for all regions.

The final assessment model options correspond to a combination of model configurations, including alternative assumptions on growth (otolith or spine based age estimates), alternative values of SRR steepness (0.7, 0.8, or 0.9), recruitment variability σ_R (0.2 or 0.4), and the alternative sample size of length composition data (20 or 5). The model ensemble (a total of 24 models) encompass a range of stock trajectories. Estimates of stock status were combined across from the 24 models and incorporated uncertainty estimates from both within and across the model ensemble.

The overall stock status estimates do not differ substantially from the previous assessment. Fishing mortality rates have remained relatively stable in recent years and are well below the F_{MSY}. Biomass was estimated to have been increasing since 2010. Spawning stock biomass in 2018 was estimated to be 42% of the unfished levels and 170% of the level that can support MSY ($SSB_{2018}/SSB_{MSY} = 1.75$). With high likelihood, current fishing mortality was estimated to be lower than F_{MSY} ($F_{2018}/F_{MSY} = 0.6$). The probability of the stock being currently in the green Kobe quadrant is estimated to over 95%. Considering the quantified uncertainty, the stock is considered not to be overfished and is not subject to overfishing in 2018. The retrospective analysis provided some confidence on the robustness of the model with respect to recent data, yet the uncertainly on levels of most recent recruitment may undermine the predictive capabilities of the model. Annual catches since the 1990s have been within the range of the estimated MSY and the current catch is projected to be sustainable over the longer term. the estimated stock status is summarized as below:

- Catch in 2018:   30 600
- Average catch 2014–2018:   30 686
- MSY (1000 t) (80% CI):   33 (27 –40)
- F_{MSY} 0.23 (0.15–0.31)
- SB_0 (1000 t) (80% CI):   250 (210–295)
- SB_{2018} (1000 t) (80% CI):   102 (70–138)
- SB_{MSY} 59 (41–77)
- SB_{2018}/SB_0 (80% CI): 0.42 (0.36–0.47)
- SB_{2018}/SSB_{MSY} 1.75 (1.28–2.35)
- F_{2018}/F_{MSY} 0.60 (0.40–0.83)

1. INTRODUCTION

This paper presents a preliminary stock assessment of Swordfish (*Xiphias gladius*) in the Indian Ocean (IO) including fishery data up to 2018. The assessment implements an age- and spatially structured population model using the Stock Synthesis 3.30 (Methot et al. 2020, Methot & Wetzel 2013).

A number of surplus production models were fitted to Indian Ocean broadbill swordfish catch and CPUE data as a first attempt at a formal model-based stock assessment at the 5th IOTC Working Party on Billfish (Anon. 2006). These models yielded plausible inferences about the impact of the swordfish fishery on the whole of the Indian Ocean population.

Kolody (2009) conducted preliminary work toward an Indian Ocean swordfish stock assessment using Stock Synthesis 3. The prime motivation for developing the SS3 model in 2009 was to increase the resolution of spatial processes, so that the differential and possibly elevated depletion in the SW Indian Ocean could be more explicitly described. The model population was age-structured, sex explicit, and spatially disaggregated into 4 regions. Kolody (2010, 2011) updated the assessment, with a focus on the SW region where a separate model was run assuming that the SW constituted a separate stock.

Sharma & Herrera (2014) updated the assessment for the Indian Ocean Model. Based on evidence of Muths et al. (2013), there are no differences in genetic structure obtained from the SW Region and the entire IO Region. As such, only one stock assessment was examined. The assessment in 2017 also adopted the one-stock hypothesis but explored several spatial structures including sub-regional models to characterise regional abundance distribution (Fu 2017).

This report provides an updated stock assessment for swordfish in the Indian Ocean using fishery data up to 2018, and builds on the work by Fu (2017), Sharma & Herrera (2014), and Kolody (2010, 2011), assuming a single Indian Ocean population stock (IO), but spatially disaggregated into four areas (Figure 1). The model incorporates the following updates:

- Three additional year of data (2016–2018),
- Improved information on nominal catches and catch and effort data from IOTC database
- Revised CPUE series for the Japanese, Taiwanese, Portuguese, Spanish, and Indonesian fleet
- Addition of the South African CPUE in the South-west (SW) region,

The assessment provides estimates of stock status and reference management quantities. Model uncertainties are characterised under combinations of model assumptions and parameter values using a grid approach. The assessment also examined a new approach to derive the regional weighting assumption based on the Japanese catch effort data.
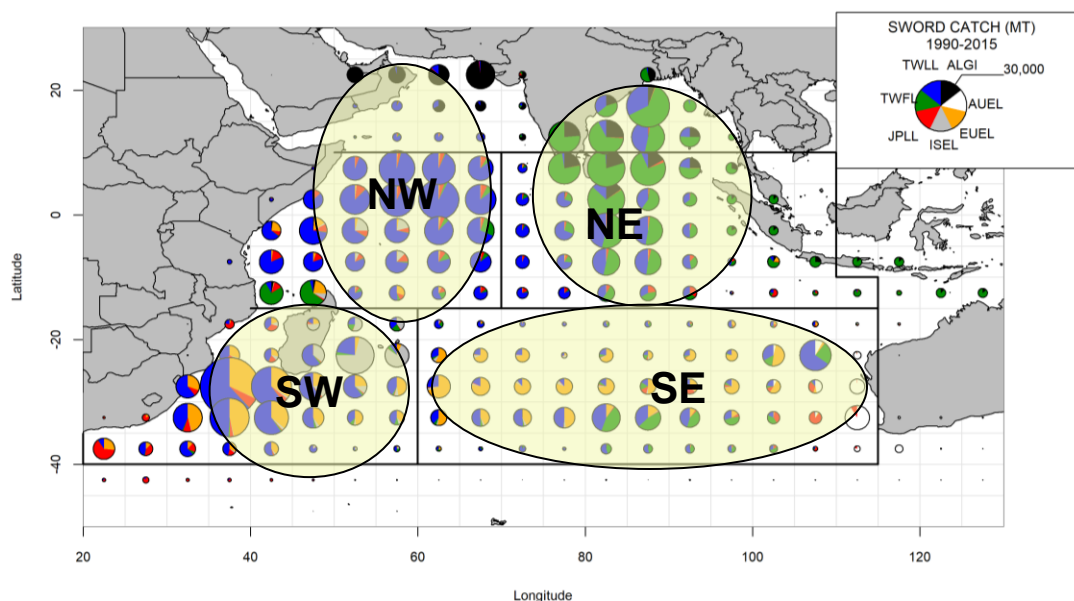
Figure 1: Spatial structure showing the 4 areas used in the assessment model, and distribution of SWO catches in the Indian Ocean by fleet aggregated for 1990-2018.

1.1 Biology and stock structure

Swordfish (*Xiphias gladius*) are a large pelagic species, broadly distributed throughout the Indian Ocean to a southern limit of 50° S. Swordfish are highly fecund, migratory fish that grow quickly in the early years and reach their maximum size at about 15 years of age. Swordfish have a wider geographical distribution than other billfish. They routinely move between surface waters and great depths and do not form schools. Female swordfish grow faster and live longer than males, and they have different distributions depending on size. There is evidence for spatial heterogeneity in size/sex composition in other oceans (Ward and Elscot 2000). Larger, predominantly female fish are observed in the more southern latitudes of the South Pacific. In Atlantic, medium and large-sized swordfish tend to dominate longline catches in temperate waters and smaller swordfish are more common in warmer waters.

Swordfish are considered batch spawners. One estimate suggested that female swordfish in equatorial waters may spawn as frequent as once every three days over a period of seven month (Ward & Elscot 2000). Swordfish larvae seem to be rare in eastern Indian Ocean. However, a few swordfish larvae have been reported from the Mozambique Channel and east of Madagascar. By contrast high concentrations occur in the north-east Indian Ocean (off north western Australia and south-west of Java) and in equatorial waters to about 80E (Ward & Elscot 2000).

Stock structure of Indian Ocean samples of swordfish were examined using genetic analyses. Lu et al. (2006) describe mitochondrial DNA evidence for three possible population delineations within the Indian Ocean (but recognised that increased sample sizes would be desirable), suggesting samples drawn from the waters off northern Madagascar and the Bay of Bengal were 2 distinct groups compared to the other populations from the Indian Ocean and West Pacific. In the Indian Ocean, a large continuous larval distribution in the eastern Indian Ocean is described in Nishikawa et al (1985). Unfortunately, other regions of the Indian Ocean were not as heavily sampled. Some evidence suggests that there may be genetic distinction within the IO, and this is the subject of ongoing investigation of the IOSSS project led by IFREMER, Reunion (Bradman et al. 2010. Bourjea et al 2011). Results obtained in 2013 (WPB 2013, Muths et al. 2013) did not identify any clear differences in genetic structure within this ocean, suggesting it is appropriate to consider swordfish as a single population in the Indian Ocean.

1.2 Fishery overview

Indian Ocean swordfish have been taken by the Japanese longline fleet primarily as by-catch, since the early 1950s (Figure 2). The population was not heavily exploited before targeted fisheries began in the early 1990s. At this time the Taiwanese longliners began taking large numbers, initially in the SW region, followed by the other regions. As the Fresh Tuna longline fishery developed in the late 1980s, annual catches rapidly increased to reach a peak of about 35,000 in the late 1990s–early 2000s. The European longline fleet (predominantly from Spain) started a targeted fishery in the 1990s, while only small numbers are reported in the driftnet fisheries, and purse seine catches are very rare. Total catches have declined substantially since the mid-2000s, attributed to large effort decreases in the longline fleets due to risk of piracy). Since 2012 catches appear to show signs of recovery as a consequence of improvements in security in the area off Somalia. Swordfish are a high value catch that represent an increasingly important source to many coastal nations in Indian Ocean.
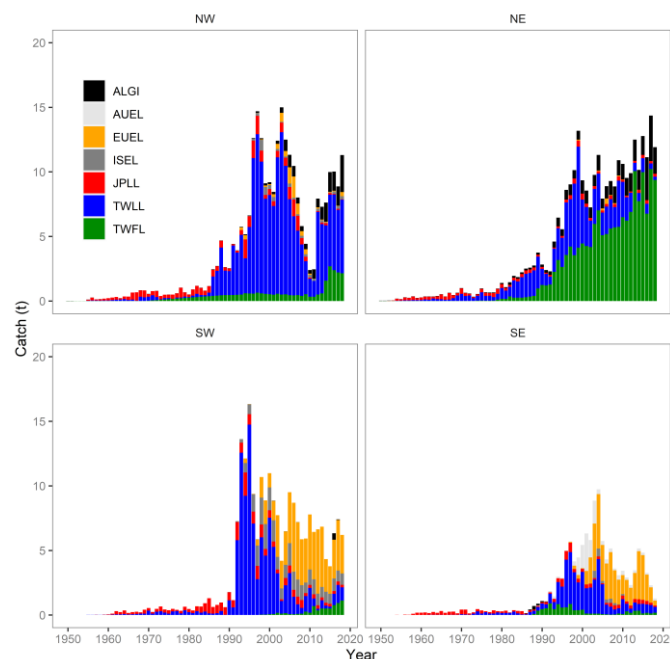

Figure 2: Total swordfish catch in tonnes by fishery fleet over time for the North-west (NW), North-east (NE), South-west (SW), and South-east (SE) regions in the Indian Ocean.

2. OBSERVATIONS AND MODEL INPUTS

The data used in the swordfish assessment consist of catch and length composition data for the fisheries defined in the analysis, and regional longline CPUE indices. The details of the configuration of the fishery specific data sets are described below.

2.1 Spatial stratification

The appropriate spatial structure for the assessment remains uncertain. Different hypotheses have been proposed, various options have been explored for IO swordfish to date, including (1) one or more discrete stocks (2) two or more populations that are produced from a common spawning ground, but have foraging grounds site fidelity (i.e. while this is a single population genetically, depletion can differ in different regions at different rates) 3) discrete spawning populations with mixing in common foraging grounds.

Some evidence suggests that there may be genetic distinction within the IO (Bradman et al. 2010, Bourjea et al 2011). Based on results obtained in 2013 (Muths 2013), there are no differences in genetic structure obtained from the SW Region and the entire IO Region. As such, the assessment is based on the single stock IO model (Shared spawning with foraging grounds site fidelity). However, the model is disaggregated into 4 areas corresponding to those used in the Japanese and Taiwanese catch rate standardization analyses in recent years (Figure 1). Given the vast size of the Indian Ocean, and the migration rate inferences that have been made from tagging studies to date, it seems unlikely that there would be rapid mixing processes across the whole basin, even if the population was genetically homogeneous. As such, localised overfishing could result in negative local consequences even if the population is genetically homogenous. The 4-area structure is a pragmatic disaggregation that conveniently partitions most of the national fleets.

SS3 can estimate movement rates among areas, however, these estimates are generally of little value in the absence of tagging data. In all models, migration rates were fixed at very low levels (<< 1% per year), which essentially creates 4 populations except for the shared spawning and recruitment dynamics (foraging grounds site-fidelity).

The previous assessment also developed sub-regional models in which each region was assumed to be a single stock and each model was fitted only to the region-specific data. However, the sub-regional models were mainly to derive weighing factors for determining biomass distributions in a spatially disaggregated IO model.

2.2 Definition of fisheries

There are many different fisheries catching swordfish in the Indian Ocean (see below), with vastly different gear types and levels of data quality (IOTC 2020):

- ALGI – Gillnet, trolling and other minor artisanal fisheries
- AUEL – Longline fishery of Australia (target is SWO)
- EUEL – EU longliners targeting SWO plus other longliners assimilated to EU longliners
- ISEL – Semi-industrial longline fleets operating in Reunion (EU.France), Mayotte (EU.France), Madagascar, Mauritius and the Seychelles
- JPLL – Longline fishery of Japan plus other fleets assimilated to the Japanese fleet
- TWLL – Large scale tuna longline fleet of Taiwan,China, plus other longline fleets assimilated to the Taiwanese fleet
- TWFL – Fresh-tuna longline fleets of Taiwan and Indonesia, plus other fresh-tuna longline fleets assimilated to those

For the assessment, 15 fleets were defined based on spatial disaggregation of these fisheries (Table 1). This differs somewhat to the simplification made in the previous assessment which aggregated the longline fleets as one homogeneous fishery group in each region except for SW. However, preliminary investigations suggested that there are somewhat differences in the size compositions of samples taken by the longline fleets (e.g. the JPLL fishery tend to catch more large fish) which potentially indicate differential selectivity patterns amongst the fisheries. Therefore, the current assessment maintained the disaggregation of the fleet structure for the longline fisheries.

Table 1: Fleet definitions (number 1–15) and for the SS3 Assessment. Suffixes denote regions within the Indian Ocean as indicated in Figure 1: NW – North-West; NE – North-East; SW – South-West; SE – South-East.

Name	number	Area	Description
ALGI_NW	1	NW	Northwest Gillnet and other non-longline/-handline gears
JPLL_NW	2	NW	Northwest Japan and assimilated longliners (target tunas)
TWLL_NW	3	NW	Northwest Taiwan,China and assimilated longliners and handlines (mixed target)
ALGI_NE	4	NE	Northeast Gillnet and other non-longline/-handline gears
JPLL_NE	5	NE	Northeast Japan and assimilated longliners (target tunas)
TWLL_NE	6	NE	Northeast Taiwan,China and assimilated longliners and handlines (mixed target)
TWFL_NE	7	NE	Northeast fresh-tuna longliners (target tunas)
EUEL_SW	8	SW	Southwest European and assimilated longliners (target SWO)
ISEL_SW	9	SW	Southwest semi-industrial longliners (target SWO)
JPLL_SW	10	SW	Southwest Japan and assimilated longliners (target tunas)
TWLL_SW	11	SW	Southwest Taiwan,China and assimilated longliners and handlines (mixed target)
AUEL_SE	12	SE	Southeast Australia Longline fishery of Australia
EUEL_SE	13	SE	Southeast Southeast west European and assimilated longliners (target SWO)
JPLL_SE	14	SE	Southeast Japan and assimilated longliners (target tunas)
TWLL_SE	15	SE	Southeast Taiwan,China and assimilated longliners and handlines (mixed target)

2.3 Catch history

Catch data were compiled based on the fisheries definitions (Figure 3). An update of catches by fishery was provided by the IOTC Secretariat, including catches from 2016–2018. The time series of catches were similar to the catch series included in the 2017 assessment except for the fresh longline fisheries, as a result of the revision to the the Indonesia's fresh longline catches. The revision incorporated changes to IOTC Secretariat's catch estimation methodology that led to Indonesia's fresh longline catches of swordfish being revised down from over 50,000 t to less than 35,000 t in recent years (Geehan 2018, Geehan & SETYADJI 2018). There are also some major revisions to the swordfish catches from I.R. Iran and Pakistan's gillnet fishery (IOTC–2019–WPB17–07). Overall, the longline catches currently comprise around 70% of total swordfish catches in the Indian Ocean.
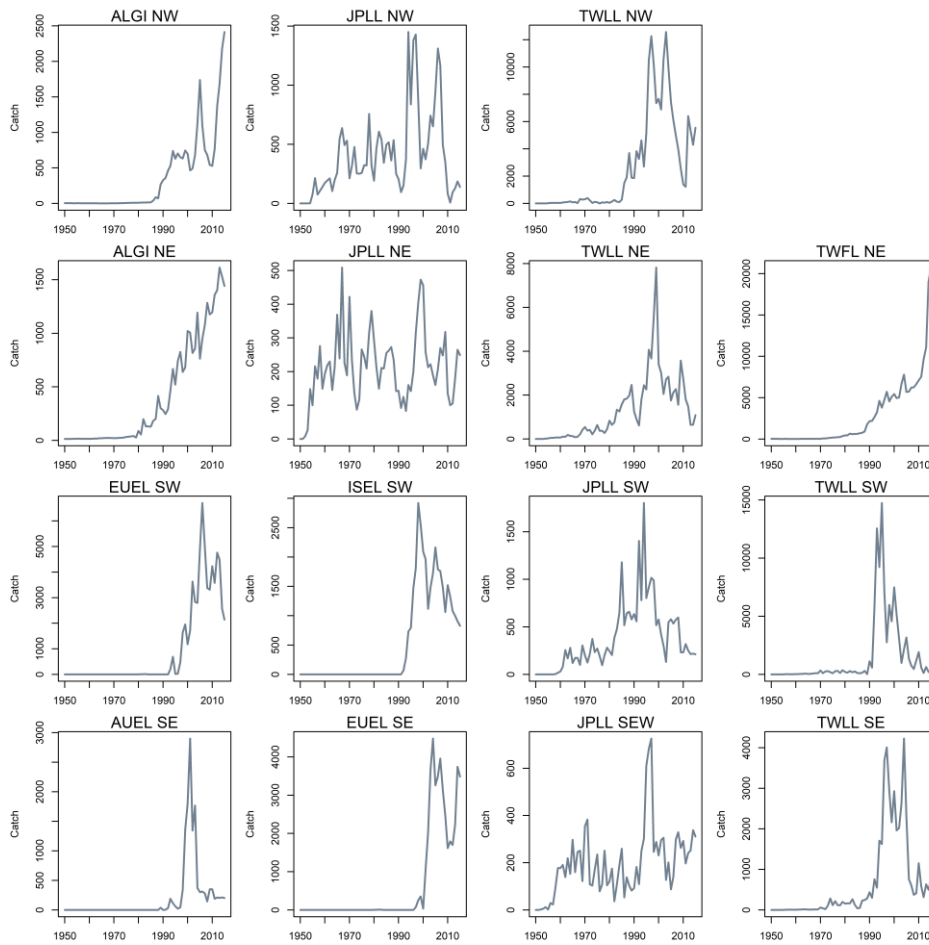
Figure 3: Fishery catches (metric tonnes) aggregated by year. Note the y-axis differs among plots.

2.4 CPUE indices

Thirteen standardized CPUE series (Table 2, Figure 4) were submitted to WPB for the assessment, including the Japanese (Taki et al. 2020), Taiwanese (Wang 2020), Spanish (Cartelle 2020), Portuguese (Coelho & Rosa 2020), South African (Parker & Kerwath 2020), and Indonesian (Setyadjy et al. 2020) fleets. The CPUE series are included in the assessment as relative abundance indices.

In each region, the Japanese CPUE series were standardised as two separate series: 1979–1993 and 1994–2018, because there were the significant differences between the two periods in terms of hooks between Floats, proportion of zero-catch sets and targeting practices (Taki et al. 2020).

In each region, the Taiwanese indices were standardised for 1979 to 2019 (the index in 2019 was not used). In most areas, the early indices exhibited some large fluctuations, which can hardly be explained by the population dynamics. Some of the fishing practices for swordfish by longliners (the use of squid baits with light sticks, setting shallower at night) were widely adopted in the late 1980s, probably resulted in significant improvements in swordfish catch rates (Campbell 1998). Thus, the Taiwanese CPUE is also considered as two separate series: 1979–1993 and 1994–2018 in each region.

The Portuguese pelagic longline fishery in the Indian Ocean started in the late 1990's, targeting mainly swordfish in the southwest, also catches relatively high quantities of sharks as bycatch in certain areas and seasons (Coelho & Rosa 2020). The Portuguese series showed a declining trend between 2000 and 2018. The index is assigned to the SW region in the assessment model.

The Spanish series from 2000 to 2018 is also assigned to the SW region although the fleet has fished a much larger area. Shifting targeting (i.e. shark vs swordfish) is very important in this fishery. Earlier analysis demonstrated that the inclusion or exclusion of the species ratio factor makes very little difference to the annual time series in this case, suggesting that the seasonal targeting shifts are probably not introducing any consistent bias to the time series.

The South African Series is based on a Swordfish target fishery of the South African pelagic longline fleet operating along the west and east coast of South Africa. The South African index showed a declining trend between 2006 and 2018, in a magnitude similar to the Portuguese CPUE. The index is assigned to the SW region in the assessment model.

The Indonesian CPUE series derived from observer data covering 2006 to 2018 is assigned to the NE region. The index appears to be very noisy but has an overall flat trend.

The CPUE series from the different longline fleets suggest very different abundance trends. In the NW, Japanese indices show a large decline since the mid-1990s the Taiwanese indices show an overall flat trend; in the SE, Japanese CPUE had a steeper decline than Taiwanese CPUE; In the NE, Japanese and Taiwanese CPUE show opposite trends. In the SW, Japanese CPUE is sharply increasing, Taiwanese CPUE series is steeply decreasing, yet the Spanish index is relatively stable. Some of these conflicts could be attributed to the over-interpretation of noise.

There is considerable variability in recent Japanese CPUE indices. There has been a large reduction of effort by the Japanese longline fleet since 2005, coinciding with the onset of the piracy activity in the western Indian Ocean. The reduction of fishing mostly occurred in the north west Indian Ocean as the Japanese fleet pulled out of the region but is also evident in other regions. Although the piracy activity has abated after 2012, the effort has not returned to the previous levels. As such, the spatial overage of the Japanese CPUE may have been poor in recent years, particularly in the NW and NE regions.

Table 2: CPUE series available for the SS3 Assessment. Suffixes denote regions within the Indian Ocean as indicated in Figure 1: NW – North-West; NE – North-East; SW – South-West; SE – South-East. Number is the SS3 index number

Name	Number	Area	Description
UJPLL_NW	16	NW	JPN CPUE series (1994-2018)
UJPLL_NE	17	NE	JPN CPUE series (1994-2018)
UJPLL_SW	18	SW	JPN CPUE series (1994-2018)
UJPLL_SE	19	SE	JPN CPUE series (1994-2018)
UTWLL_NW	20	NW	TWN CPUE series (1994–2018)
UTWLL_NE	21	NE	TWN CPUE series (1994–2018)
UTWLL_SW	22	SW	TWN CPUE series (1994–2018)
UTWLL_SE	23	SE	TWN CPUE series (1994–2018)
UPOR_SW	24	SW	POR CPUE series (2000–2018)
UESP_SW	25	SW	ESP CPUE series (2000–2018)
UZAF_SW	26	SW	ZAF CPUE series (2004-2018)
UREL_SW	27	SW	REL CPUE series (1994-2018)
UIND_NE	28	NE	IND CPUE series (2006-2018)
UJPLL_NW	29	NW	*JPN CPUE series (1979-1993)
UJPLL_NE	30	NE	*JPN CPUE series (1979-1993)
UJPLL_SW	31	SW	*JPN CPUE series (1979-1993)
UJPLL_SE	32	SE	*JPN CPUE series (1979-1993)
UTWLL_NW	33	NW	**TWN CPUE series (1979–2015)
UTWLL_NE	34	NE	**TWN CPUE series (1979–2015)
UTWLL_SW	35	SW	**TWN CPUE series (1979–2015)
UTWLL_SE	36	SE	**TWN CPUE series (1979–2015)

* JPN CPUE series were standardised for 1976–1993 and 1994–2015 separately.
** TWN CPUE series were treated as two separate series: 1979–1993 and 1994–2015 in the assessment
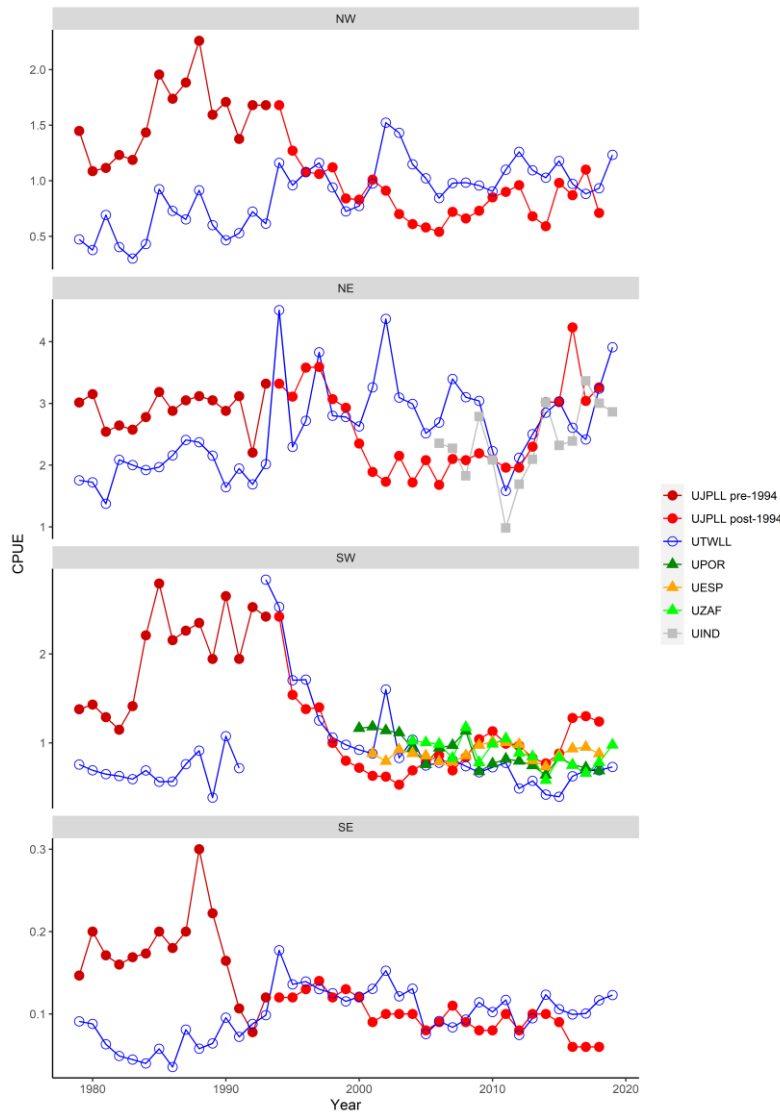
Figure 4: Standardized CPUE by area for Japanese, Taiwanese, Portuguese, Spanish, South African, and Indonesian longline fleets by sub-region based on papers submitted to WPB18. All series have been rescaled so that they are visually comparable for relevant periods of overlap. Note that this re-scaling does not reflect the relative weighting that is applied to the Japanese fleet. Also note that Japanese indices were standardised for 1979–1993 and 1994–2018 separately, and Taiwanese CPUE series were treated as two separate series: 1979–1993 and 1994–2018 in the assessment.

2.5 Length frequency data

Length-frequency observations are available for 14 of the 15 defined fisheries (except for the gillnet fishery in the NW). Size composition was partitioned into 25 bins of width 9 cm (except the first and last), from <45cm to >252 cm). The length frequency observation for each fishery represents the actual number of swordfish measured. In the assessment, all length composition strata from all fleets were down weighted by dividing the number of fish included in the aggregated sample by a factor of 10, with a maximum sample size of 20, to account for sampling is probably not truly random. Explorations from the previous assessment suggested that this weighting option is consistent with the effective sample sizes determined using the Francis (2012) method. Aggregated size distributions and time series of mean size are shown in Figure 5 andFigure 6, respectively.

There is some noticeable difference in size compositions amongst the fleets and the Japanese fleet appears to have caught more larger swordfish, which is evident in the overall wider size distribution from the JPLL catch samples (Figure 5). The trends also differed among longline fleets in some areas,

e.g. the average fish size from the Japanese and the EU longline size data show a somewhat declining trend in recent years, whereas the Taiwanese and Seychelles data show a significant increase (Figure 6). According to Herrera and Pierre (2014), most samples available from the longline fishery of Japan come from training vessels in recent years. The representativeness of the samples collected on training vessels is uncertain, as these vessels do not necessarily operate in the same areas or use the same fishing techniques as the commercial vessels from Japan.
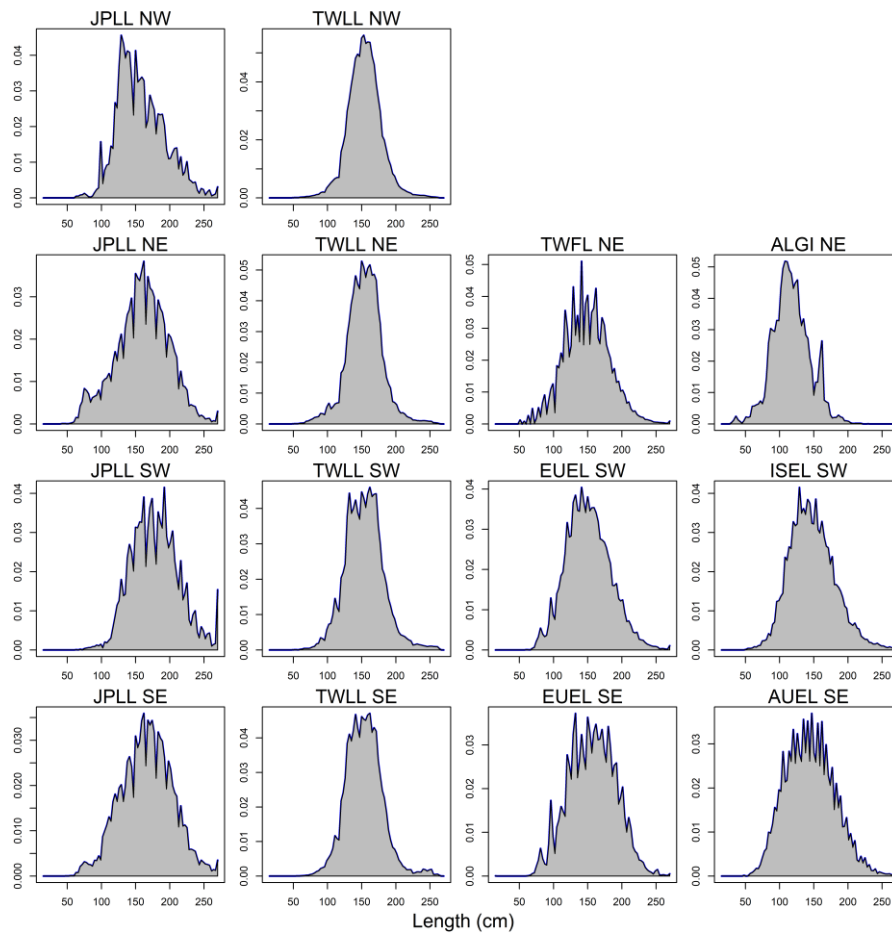

Figure 5: Length compositions of swordfish samples aggregated by fishery.
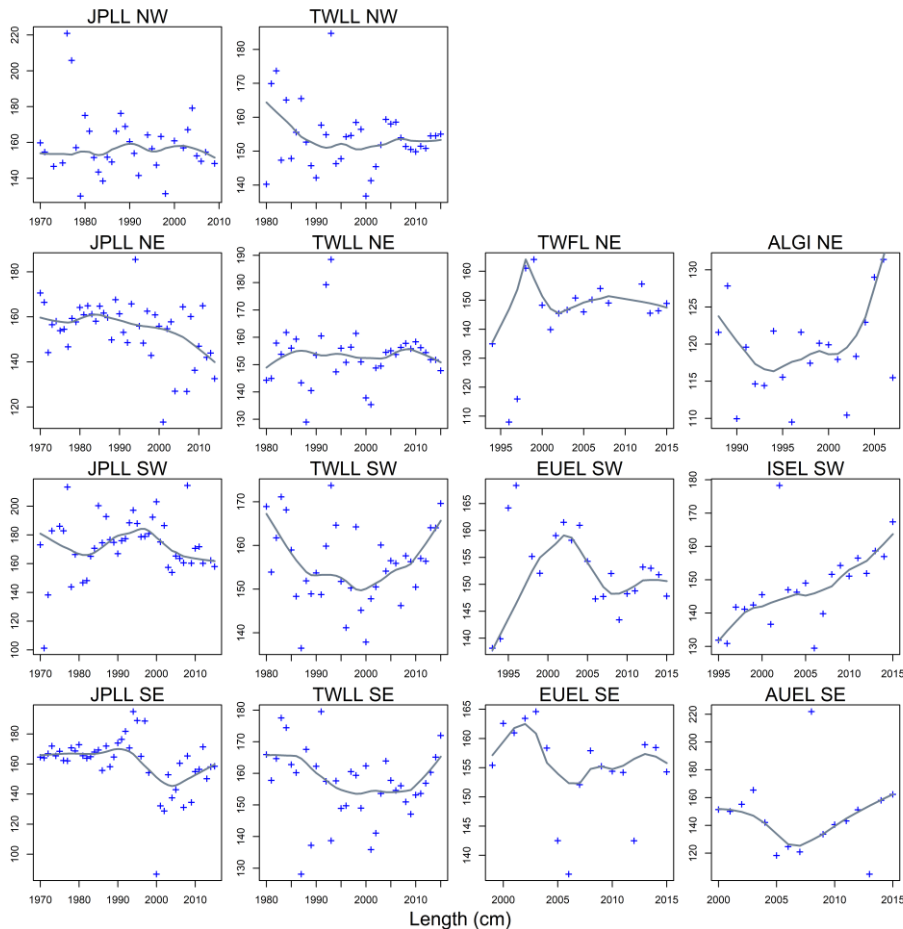
Figure 6: Mean length (fork length, cm) of swordfish sampled from the principal fisheries by year quarter. The grey line represents the fit of a loess smoother to each dataset.

3. MODEL STRUCTURAL AND ASSUMPTIONS

3.1 Population dynamics

The stock assessment model partitioned the Indian Ocean swordfish population into four areas, two sex groups, and age groups 1–30 years with the last age a plus group (in unfished equilibrium, <0.25% of the population survives to reach the plus-group with the M value considered).

The swordfish population is sex-structured to (potentially) account for a number of sex-specific population features that may be worth describing. Notably, growth curves differ by sex, and it is useful to be able to represent the two distributions (or aggregated of the two distributions) in the catch-at-length likelihoods (or it would be useful in principle, if we were confident about the growth curves, size composition data, mortality estimates and stationary selectivity assumptions). Spatial distributions often differ by sex (e.g. large females are disproportionately found in cooler temperate waters in the south Pacific). Selectivity may differ by sex due to the differing spatial distributions, and there also may be direct size biases in some fisheries (e.g. commercial fishers report that large swordfish may be less vulnerable to circle hooks). Natural mortality may also be sex-specific, but no distinction was made in these models. However, there is no evidence that the sex structure is contributing much to the behaviour of the model in its current form.

The population was assumed to be in unfished equilibrium in 1950, the start of the catch data series. The model was iterated from 1950-2018 using an annual time-step. The nominal unit of time in the model is one year during which population processes (e.g., recruitment, spawning, and ageing) were

13

applied in sequence according to the dynamics implemented within the Stock Synthesis model (Methot 2020). Observations were fitted to model predictions within the year. The main population dynamics processes are as follows:

3.1.1 Recruitment

Recruitment was assumed to occur annually at the start of the year. New recruits enter the population as age-class 1 fish (averaging approximately 70 cm). Annual recruitment deviates from the recruitment relationship were estimated in the model for 1970–2017 (48 deviates). The recruitment deviates were estimated for the period that may be informative regarding the variation in recruitment. Recruit in the final year was deterministic from the stock recruitment relationship (because these cohorts are only weakly observed by the data). The final model options included three (fixed) values of steepness of the BH SRR (h 0.7, 0.8 and 0.9).

Recruitment deviates were assumed to have a standard deviation (σ_R) of 0.2, with an alternative value of 0.4 also included in the final model options. There is anecdotal evidence to suggest that spawning (and recruitment) may be out of phase in the southern and northern hemispheres, however, the growth, size sampling and selectivity assumptions are such that the quarterly model explored in 2010 could not provide much insight into recruitment processes. Swordfish are often assumed to have lower recruitment variability than tuna populations, and the recent summary of tuna populations suggest that the estimated (annual) variability is often lower than has been a priori assumed in the tuna assessments (ISSF 2011 reports values of 0.2 – 0.5).

Area-specific parameters were estimated to distribute the mean recruitment among regions. Recruitment anomalies by region were estimated with a very high CV, such that the spatial distribution of recruits was only indirectly constrained by the overall recruitment CV.

3.1.2 Growth and maturity

Swordfish exhibit phenomenal growth in the first year of life and there is a marked difference in growth rate between male and female. The strong evidence for sex dimorphism in swordfish can be potentially important in the right-hand tail of the size distribution, which is often estimated to consist predominantly of large mature females. The previous assessment considered four alternative sets of growth curves to allow for uncertainty due to potential area-specific growth rates, and ongoing concerns about age estimation from fin spines.

- CSIRO estimated very slow growth based on South-East Indian Ocean fin ray samples (Young and Drake 2004).
- NMFS estimated higher growth from Hawaiian samples (DeMartini et al. 2007).
- Wang et al. (2010) described an intermediate growth curve (pooled western and eastern samples from the Indian Ocean equatorial region).
- New CSIRO estimates based on SW pacific fin ray samples (Farley el al. 2016).
- New CSIRO estimates based on SW pacific otolith samples (Farley el al. 2016).

Farley et al. (2016) undertook a growth study for swordfish in South-West Pacific waters comparing the use of both fin-rays and otoliths samples. The study found that age estimates from fin rays and otoliths produce different growth curves in the SW Pacific, with discrepancies evident in age classes >7 years for females and >4 years for males. The otolith-based growth curves indicate slower growth and a higher maximum age for both males and females, compared to the ray-based growth curves of Young & Drake (2004) and DeMartini et al. (2007). Although direct validation of the ageing method was not carried out in the study, age estimates from otoliths are likely to be more reliable than fin- rays, especially in larger/older fish, as fin-rays are subject to resorption and vascularisation of the core (Farley et al. 2016). The study also suggested that estimated ages for larger fish are older when derived from otoliths and the close correspondence of the new growth curves with those from Hawaii. Consequently,

the WPB15 agreed that the stock assessment for swordfish should use the new otolith-based estimates from Farley et al. (2016) (**Figure 7** – left). Following the previous assessment, the Taiwan estimate (Wang et al. 2010) was also included in final model options.

Length-at-age was assumed to be normally distributed around the mean length-at-age relationship with a CV of 15% at age 0, decreasing linearly (in proportion to length) to 10% at age 30+.

While a number of studies quantify the relationship between size and maturity, the uncertainty of age estimation that undermines the growth relationships also undermines the maturity/fecundity by age relationship. Following recommendations from WPB15, the assessment used the age-based logistic ogive from Farley et al. (2016) (as applied from the new otolith-based growth from SW pacific), which suggested a 50% maturity at about age 4.34 (Figure 7 – right).
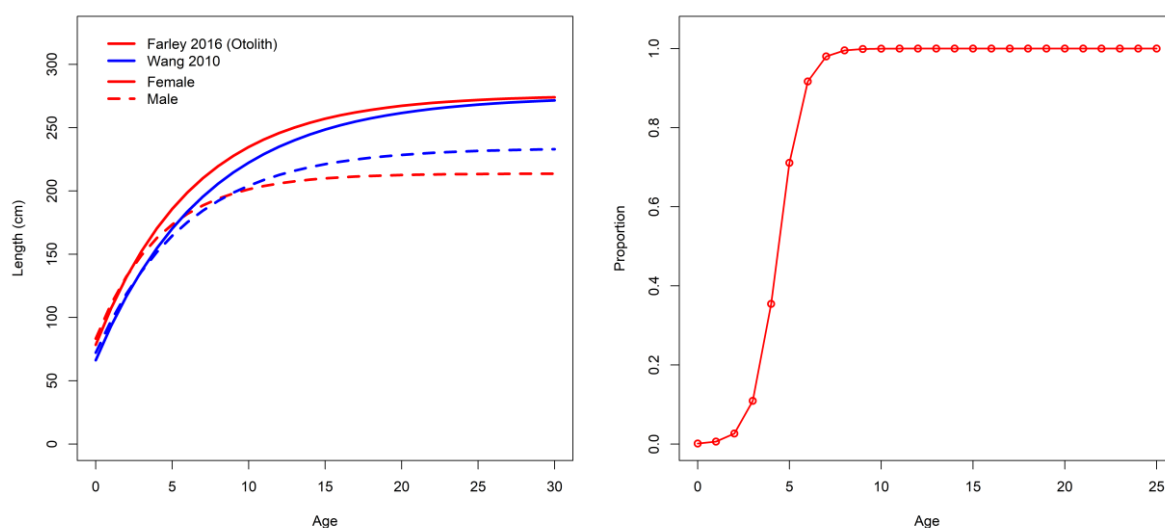

Figure 7: Growth (left) and age-based maturity (right) for swordfish. Two growth options are considered in the assessment: CSIRO SW Pacific otolith (GoMf) and Taiwan Indian Ocean (GtMf).

3.1.3 Natural mortality

Natural mortality estimates for swordfish are highly uncertain given the current methods of age estimation are poorly validated. There are a broad range of M values assumed in other swordfish assessments worldwide, ranging from at least 0.2 – 0.5 (Davies et al. 2013). The value of M=0.25 (constant over ages) was adopted for the current assessment.

3.2 Fishery dynamics

3.2.1 Selectivity

In the 2017 assessment (also in 2014 and 2011), only two different size-based "double normal" selectivity curves were estimated, one for longline fleets, and one for the gillnet (and other associated) fleets. This assumption was revisited in the current assessment and separate selectivities were estimated for a number of longline fleets, i.e., JPLL, TWLL, TWFL, and EUEL. A monotonically increasing logistic selectivity was estimated for the JPLL fishery, and a double normal selectivity for the TWLL and EUEL fisheries. The selectivities for the ISEL and AUEL were assumed to be same as the EUEL. The assumption of an asymptotic selectivity for at least one of the fisheries (i.e. JPLL) prevents the model from producing cryptic biomass. The selectivity for each fleet was shared by region (e.g. a common JPLL selectivity in the IO). A cubic spline selectivity (5 nodes) was assumed for the gillnet fishery in the NW and NE. The cubic spline selectivity has considerable freedom to represent a dome-shape, or an approximately logistic curve

that either reaches a plateau or is monotonically increasing.

Previous assessments found results were insensitive to eithers (age-based vs pseudo-length-based selectivity. Therefore, Selectivity was parameterized as a pseudo-length-based function, i.e. the length-based curve is internally converted to an age-based function based on the length-at-age relationship. In this application, the potential benefit of this arises as a result of the sex dimorphism (i.e. two sex-specific age-based selectivity functions are derived from a single length-based selectivity function because of the difference in length-at-age). While the length-based selectivity function often exhibits a very steep ('knife-edge') slope, this is deceptive because there is considerable overlap in length-at-age.

Fishing mortality was modelled using the hybrid method that estimates the harvest rate using Pope's approximation and then converts it to an approximation of the corresponding F (Methot & Wetzel 2013).

3.2.2 Catchability

Catchability was assumed to be constant over time for all CPUE series. An area-specific scaling was applied to the Japanese CPUE series to convert the indices to relative abundance indices that are comparable among areas (i.e. CPUE = 1 in the NW region and CPUE =1 in the SW region implies that the two regions have identical abundance, not simply identical density). This allows catchability to be shared among areas for regional CPUE index. The shared catchability constraint is often useful for preventing bizarre localised behaviour in spatial models

In the 2017 assessment, two alternative sets of regional scaling factor were used: one is based on the area of the region (Nishida 2008), and the other on biomass estimates from region-specific models (Fu 2017). The area-based scaling factor implies that the Japanese CPUE are essentially density estimates. However, the validity of the assumption that density is uniform within each large sub-region is questionable (it may be unrealistic to expect that swordfish catchability in a northern swordfish fishery has much relation to swordfish catchability in a southern SBT fishery). Further, changes in the CPUE standardisation methodologies have resulted in very different regional weighting being applied between assessments (see Figure 17 of Sharma (2014) and Figure 13 of Kolody (2011)). The biomass-based estimates were derived by fitting region-specific models which included only regional fishery catches and observations, and the resulting stock biomass in each region were used to provide prior information on regional abundance distribution in the spatially disaggregated IO model.

Here, we examined a set of alternative estimates for swordfish following the apporach of Hoyle and Langley (2020), which incorporated both the size of the region and the relative catch rate to estimate the relative level of exploitable longline biomass among regions. The method involves fitting a standardization model to the longline catch effort data and using the estimated spatial effects to approximiate fish density. Speciically we fitted a generalized linear model to the aggregated Japanese longline catch effort data: $\log(catch\ per\ thousand\ hooks) \sim year + month + 5*5cell$. The data were restricted to 1960 – 2010, a period with relatively stable catches and spatial coverage. The scaling factors were calculated by taking the standardised catch rate in each $5°$ grid cell, summing over all cells in each region. Estimated scaling factors for the NE, NW, SE, and SW regions are 1.11, 1.06, 1.17, and 0.67, respectively. To incorporate in the assessment model, the standardised CPUE index (JPLL and TWLL) in each region was normalised to its mean and was then scaled by the respective regional scaling factor.

3.3 Modelling methods, parameters, and likelihood

The model is conditioned on catch (weight), such that it is assumed to be known without error, and extracted perfectly. The SS3 "hybrid" fishing mortality parameterisation was used, where SS3 starts with Pope's approximation and then conducts a fixed number (4) of iterations to approximate instantaneous F from the Baranov catch equation.

Parameters were estimated by minimising the objective function consisting of the following terms:
- Likelihoods
  - Relative abundance indices with lognormal observation errors. Depending on the CPUE option, some of these CPUE series may have been down-weighted to the point that they were uninformative.
  - Length frequencies – multinomial sampling assumptions (with assumed sample sizes << reported sample sizes depending on the option)
- Prior distributions and Penalties:
  - Annual recruitment deviates (lognormal) from the stock-recruitment relationship.
  - Every estimated parameter for selectivity, catchability, and R0, requires a prior probability distribution. For these parameters, the prior adopted was very diffuse, such that a bound was likely to be hit before the prior would exert an appreciable influence (e.g. SD = 99).
  - Weak penalty (e.g. SD = 99) on the spatial distribution of the recruitment deviates in the 4 area model.
  - Smooth penalties for parameters approaching bounds were adopted, however, bounds were not approached for any of the models discussed here (i.e. presumably because the parameters that are most difficult to estimate were generally fixed (i.e. growth, M, steepness).

The informative parameters estimated by the model included:
- Catchability for the informative CPUE series
- Selectivity parameters
- Virgin recruitment
- Annual recruitment deviations from the stock recruitment relationship
- Annual area-specific recruitment deviations
- Recruitment distribution by area

The Hessian matrix computed at the mode of the posterior distribution was used to obtain estimates of the covariance matrix, which was used in combination with the Delta method to compute approximate confidence intervals for parameters of interest.

4. ASSESSMENT MODEL RUNS

The approach we have taken here is to explore a range of model assumptions and parameter configurations that would impact assessment results. A basic model was identified for diagnosing model performance. Uncertainties are quantified using a grid of models running over permutations of plausible parameters and/or assumption options. The grid approach aims to provide an approximate understanding of variability in model estimates due to assumptions in model structure, which is usually much larger than the statistical uncertainty conditional on any individual model. The assessment was conducted using the 3.30 version of the Stock Synthesis software. The stock status was reported for the terminal year of the model (i.e. 2018).

4.1 2017 model continuity run

In the 2017 assessment, no explicit base case model was chosen, and the final model options selected for management advice included 48 models with alternative assumptions on levels of steepness, growth, recruitment, and weighting on length frequency data. The model option with otolith-based growth estimates, the steepness of 0.8, recruitment σ_R of 0.2, and length composition sample size of 20 was considered as a reference model (IOTC–WPB15).

The 2017 reference model was updated sequentially to ensure a level of continuity, and to assess the influence of the additional data available. The model structure was revised to extend the model period to year 2018. Incremental changes were made to the 2017 model (see Table 3 for details).

Table 3: Description of the sequence of model runs to update the 2016 base model.

Model	Description
io4_rNTP_h80_GoMf_r2_CL020	2017 reference model
Update-1Catch	Model extended to include 2016–2018, with updated catches
Update-2LF	Revised and updated length composition data for 2016 – 2018
Update-3CPUE	Revised and updated Longline CPUE indices
Update-4MSY	Extend period of estimation for recruitment deviates (to 2017); Definition of F-age for determination of MSY (2018);

4.2 Basic and sensitivity models

On basis of the updated model, further revisions were made to attain a basic model (
Table 4), which served as a starting point for the sensitivity analysis and development of the final model grid. The basic and sensitivity models examined a range of model options related to the CPUE data series, biological parameters and model structure. The analysis complemented the suite of exploratory models conducted previously, with the aim of determining a suitable ensemble of model options to estimate stock status that captures a range of uncertainty. Table 5 provides a description of the alternative model options considered for the sensitivity analysis.

Table 4: Main structural assumptions of the swordfish basic model and details of estimated parameters. Changes to the 2017 assessment are highlighted in red.

Category	Assumptions	Parameters
Recruitment	Occurs at the start of each year as 0 age fish. Recruitment is a function of Beverton-Holt stock-recruitment relationship (SRR). Regional apportionment of recruitment to NW, NE, SW, and SE. Temporal recruitment deviates from SRR, 1970–2017. Temporal deviates in the proportion of recruitment allocated to NW, NE, SW, and SE from 1965–2017.	R_0 Norm(10,10); h = 0.80 $PropR2$ Norm(0,1.0) σ_R = 0.2. 48 deviates.
Initial population	A function of the equilibrium recruitment in each region assuming population in an initial, unexploited state in 1950.	
Age and growth	32 age-classes, with the last representing a plus group. VonBert Growth based on otolith estimates by Farley *et al* (2016). Mean weights (W_j) from the weight-length relationship $W = aL^b$.	L_∞^f = 275 L_∞^m = 213.8 K^f = 0.157 K^m = 0.235 a = 3.815 e-06, b = 3.188
Natural mortality	Constant at 0.25	
Maturity	Age specific logistic function from Farley *et al* (2016). spawning population includes female fish only.	α = -6.6, β = 1.50 (a_{50} = 4.42)
Movement	Move rates were fixed at very low levels (<< 1% per year)	
Selectivity	Length specific, constant over time. Logistic selectivity for Japanese longline fisheries, common among regions. Double normal selectivity for Taiwanese longline fisheries, common among regions Double normal selectivity for Taiwanese fresh tuna longline fisheries Double normal selectivity for EUEL, ISEL, and AUEL longline fisheries, Cubic spline (5 nodes) selectivity for Gillnet Fisheries CPUE indices mirror to principal LL selectivity.	Logistic Double Normal Five node cubic spline
Fishing mortality	Hybrid approach (method 3, see Methot & Wetzel 2013).	
CPUE indices	UJPLL 1994 – 2018 for NW, NE, and SE; UJPLL 1994 – 2003, UPOR 2000 – 2018, and UZAF 2004 – 2018 for SW; Shared Japanese regional catchability coefficient. A CV of 0.1 for all indices	Unconstrained parameter q
Length composition	Length composition for 14 out of the 15 fisheries. Multinomial error structure; Length samples assigned maximum ESS of 20.	

Table 5: Description of the sensitivity models for the 2020 assessment. Changes are relative to the basic model.

Model	Description
CPUE indices	
cpueESP	The UPOR and UZAF in the SW region replaced by the UESP 2001 – 2018
cpueTWN	The UPOR and UZAF in the SW region replaced by the UTWLL 2000 – 2018;
cpueIND	Removed UJPLL 2011– 2018 in NW and NE regions; included the UIND 2006 – 2018 in the NE region.
cpuePre	Included the UJPLL-pre (1979-1993) for all regions.
TWP	Removed all UJPLL; included UTWLL 1994 – 2018 for NW, NE, and SE; included UTWLL 1994 – 2003, UPOR 2000 – 2018, and UZAF 2004 – 2018 for SW; shared Taiwanese regional catchability coefficient.
cv20	A CV of 0.2 for all indices
region	Alternative CPUE regional scaling factors developed from catch effort data
Length composition	
CL005	Down weighting the length composition data with the sample sizes reduced to a maximum of 5.
Biological parameters	
GtMf	Growth estimates from Wang et al. (2010)
r4	Recruitment deviation $\sigma_R = 0.4$.
h70	Recruitment steepness = 0.7
h90	Recruitment steepness = 0.9

4.3 Final model assessable (grid)

On basis of the exploratory analysis, final options were configured to capture the uncertainty related to assumptions on the stock-recruitment steepness, recruitment deviations, growth, and effective sample sizes on the length composition data, which are thought to contribute to the main sources of uncertainty (Table 6). Thus, the final models involved running a full combination of options on steepness (3 values), σ_R (2 values), growth (2 options), and length composition data sample size (2 values), with a total of 24 models.

Table 6: Description of the final model options for the 2020 assessment. The final models consist of a full combination of options below, with a total of 24 models. The options adopted for the basic model is highlighted.

Model options	Description
growth	• ***GoMf* – Otolith based growth estimates by Farley et al. 2016.**
	• *GtMf* – Estimates by Wang et al. 2010.
Length composition data	• **CL20 – A maximum of 20 for the effective sample size**
	• CL05 – A maximum of 5 for the effective sample size
Recruitment variability	• ***R2* – recruitment σ_R =0.2**
	• *R4* – recruitment σ_R =0.4.
Steepness	• h70 – Stock-recruitment steepness parameter 0.7
	• **h80 – Stock-recruitment steepness parameter 0.8**
	• h90 – Stock-recruitment steepness parameter 0.9

5. MODEL RESULTS

5.1 2016 model continuity run

Updating the 2017 reference model with only the catch data yielded almost identical estimates of historical stock biomass (Figure 8), despite of the revisions being made to the catch estimates of the Gillnet fisheries (see Section 2.3). The updated CPUE (UJPLL and UPOR) also had only minor effects on the assessment model. However, the inclusion of the updated length composition data appears to have an appreciable impact on the biomass estimates, with the overall stock biomass estimated to be about 3% – 12% higher than the 2017 reference model (Figure 8). This is likely to be due to the addition of new data as well as the revisions to the historical series. Further model updates (e.g. reference years for the MSY calculation) had a small impact on model estimates (Figure 8). Overall, the updated models estimated a higher level of stock productivity but did not change the conclusion of stock status (B_{2015}/B_{msy} and F_{2015}/F_{msy}) compared to the 2017 reference model.
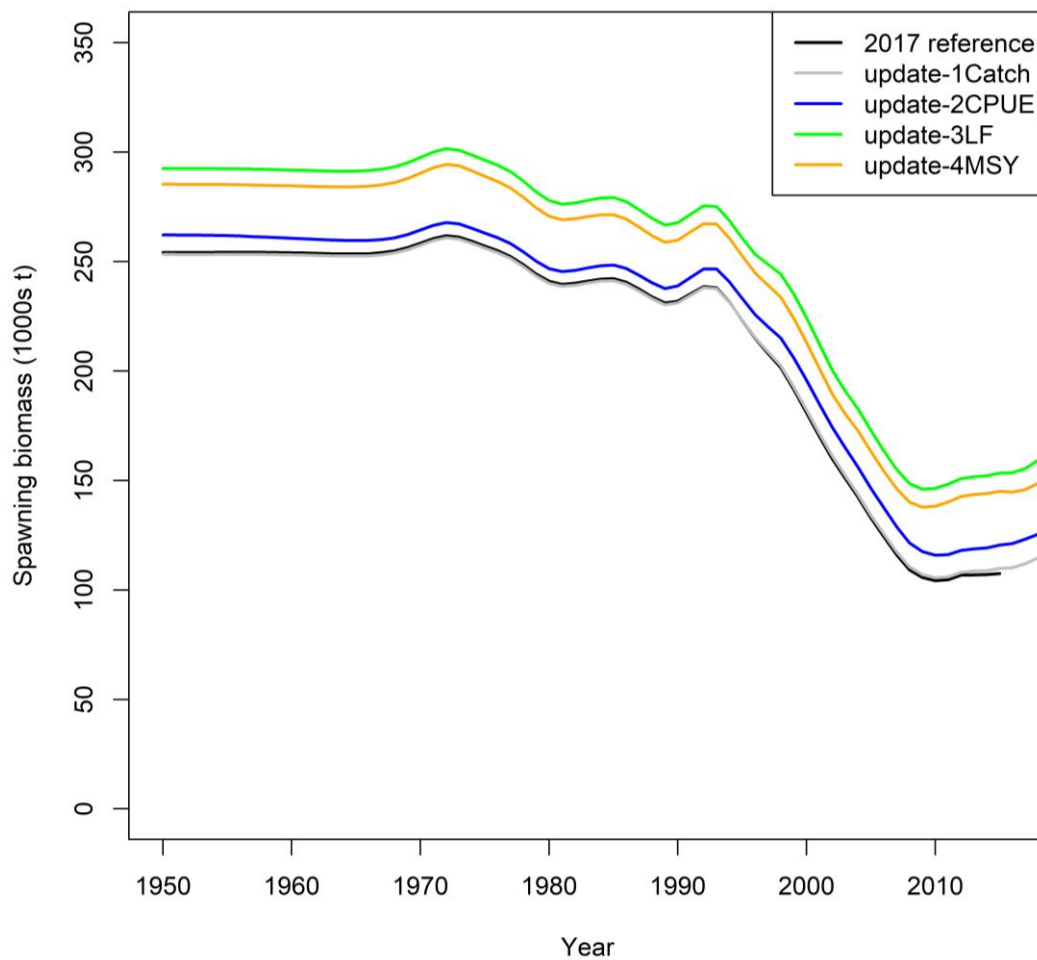

Figure 8: Spawning biomass trajectories for IO swordfish from the step-wise model updates for 2020. (from the 2017 assessment reference model '*io4_rNTP_h80_GoMf_r2_CL020*')

5.2 Basic model

On basis of the 2017 model updates, a basic model was configured (see
Table 4). The most important change in the basic model is that the fleet structure was maintained for the regional longline fisheries (instead of being amalgamated into one fishery). In addition to the UJPLL and UPOR indices as the main abundance indices, the basic model also included the UZAF index (for SW). Further, the UJPLL index in the SW was included for 1994 – 2003, overlapping with the UPOR index for 4 years (2000 – 2003), which helped to prevent some localised behaviour caused by the discontinuity of the two sets of indices (the previous assessment included UJPLL for 1994 – 1999 in the SW). The time period for which recruitment deviations were estimated was revised to include only the period 1970 – 2017, as there is no data to determine recruitment variability in the early years.

5.2.1 Model fits

The basic model was fitted to six sets of CPUE indices (4 UJPLL, UPOR, and UZAF) reasonably well (Figure 9). The decline in the UJPLL indices from the 1990s to mid-2000s is mostly driven by the significant increase of catches as well as the reduced recruitment during this period. In the SW region, the model did not fully capture by the large initial decline in the UJPLL, indicating that the extent of the decline is not entirely consistent with the model dynamics. The moderate decline in the UPOR and UZAF indices since the early 2000s was fitted well by model. In more recent years, the model also fitted well the significant increase in the UJPLL in the NE and the large decrease in the SE (as explained by divergent trends in regional recruitment). The standardised residuals show no apparent trend (Figure 10), indicating no gross misfits to these indices. Diagnostics based on the "run" test (a tool developed by Henning Winker and Felipe Carvalho) confirmed that there is generally no systematic pattern in the residuals.

The fits to the time series of annual length frequency for each of the 14 fisheries are provided in Appendix A (Figures A1–A4). Although there is no gross misfit to these data, the fits were poor in some instances (e.g. AUEL_SE 2008). The sampling may have been patchy in some fisheries in some years, with considerable variabilities in individual samples. The fits to the fleet-aggregated length frequency appear reasonable (Figure 11), indicating that the model has captured the gross features of the length composition data well (thus there is probably no significant bias in the estimates of the selectivities). The model also appeared to have tracked the mean length reasonably well – for the JPLL and EUEL fleets, the long-term trends in the predicted mean length are generally consistent with the observations (Figure 12). The model slightly over-estimated the mean length for the JPLL fleet in the NW and NE, as there is little flexibility to account for the differences in size composition among regions due to the stationary and shared selectivity assumption (for most fleets the spatial difference in length composition does not appear to be large enough to justify the adoption of region specific selectivity). Compared to the previous assessment, there is a marked improvement in the fits to the length composition from the gillnet fishery (ALGI_NE), due to the use of a more flexible selectivity form.
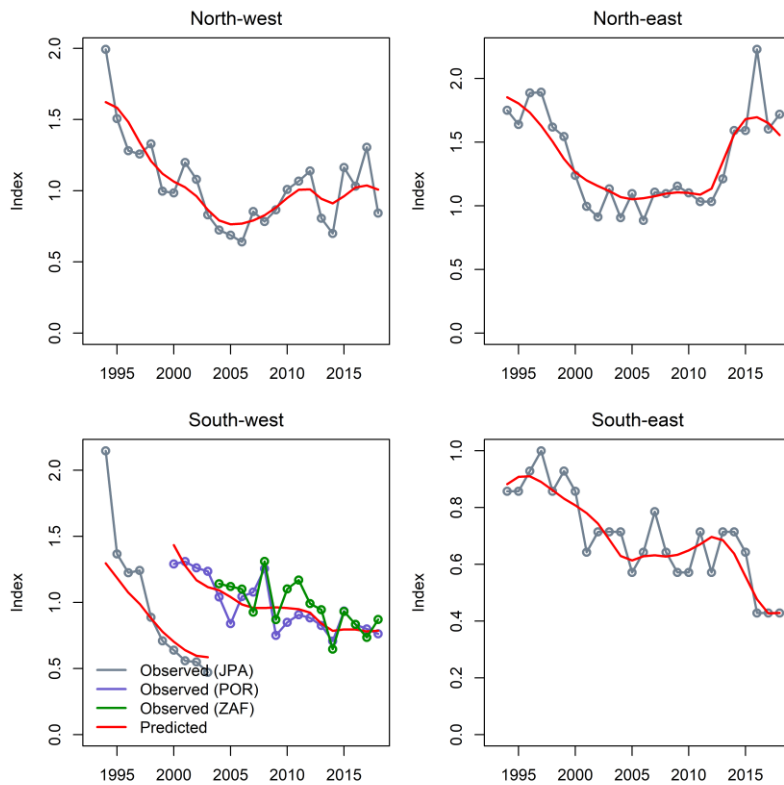
Figure 9: Fit to the regional longline CPUE indices including UJPLL 1994–2018 (except in SW 1994 – 2003), UPOR 2000 – 2018, and UZAF 2004 – 2018 from the basic model.
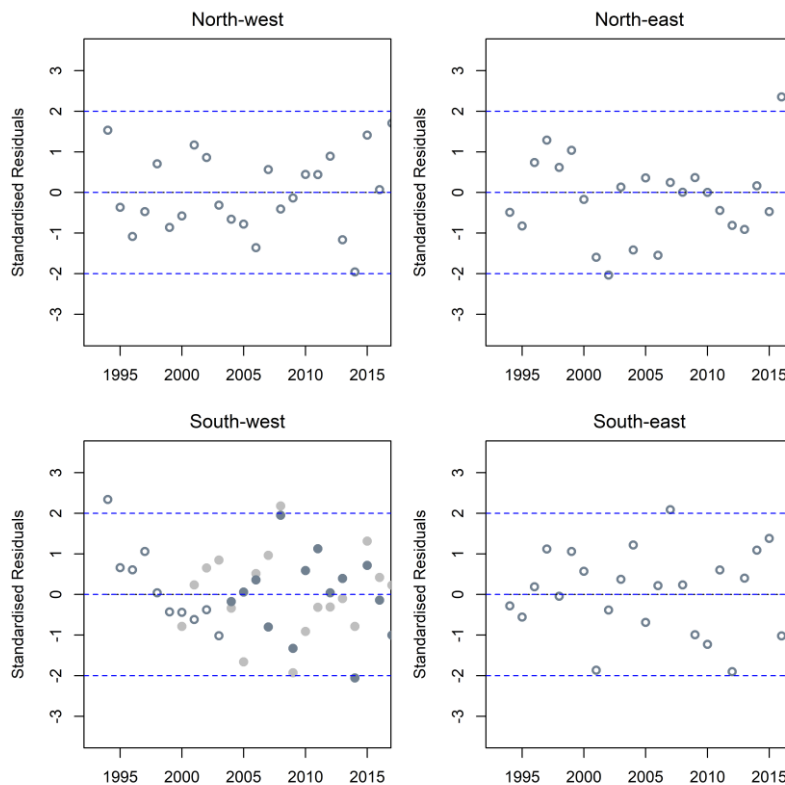

Figure 10: Standardised residuals from the fits to the CPUE indices from the basic model. Circled dots, UJPLL; light grey, UPOR; grey, UZAF.
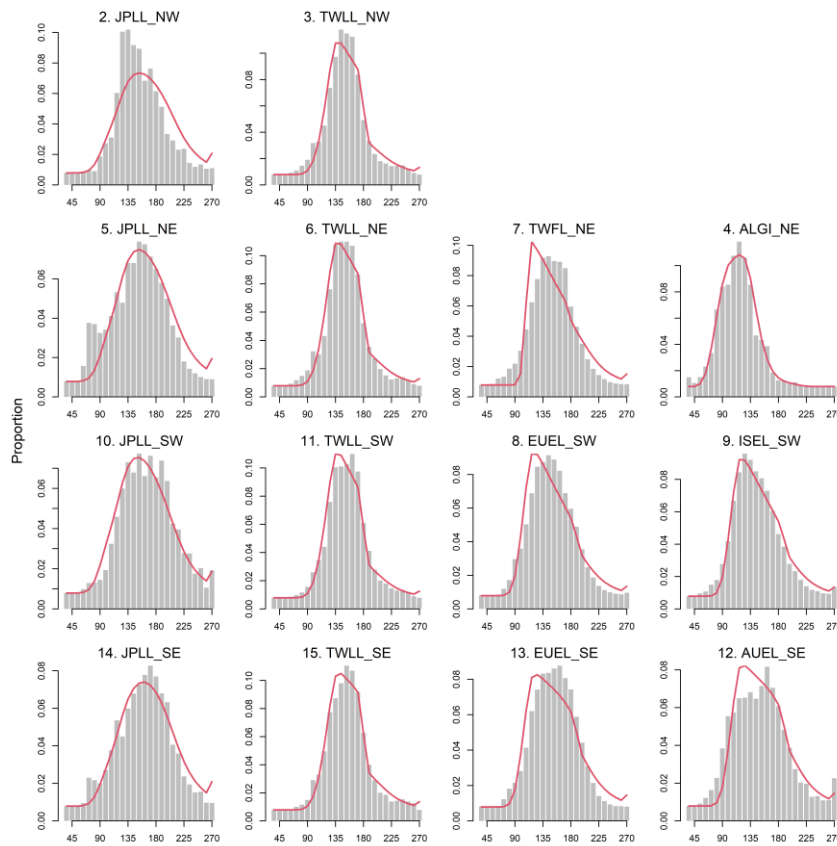
Figure 11: Observed (grey bars) and predicted (red line) length compositions (in 9 cm intervals) for each fishery of swordfish aggregated by all years for the basic model.
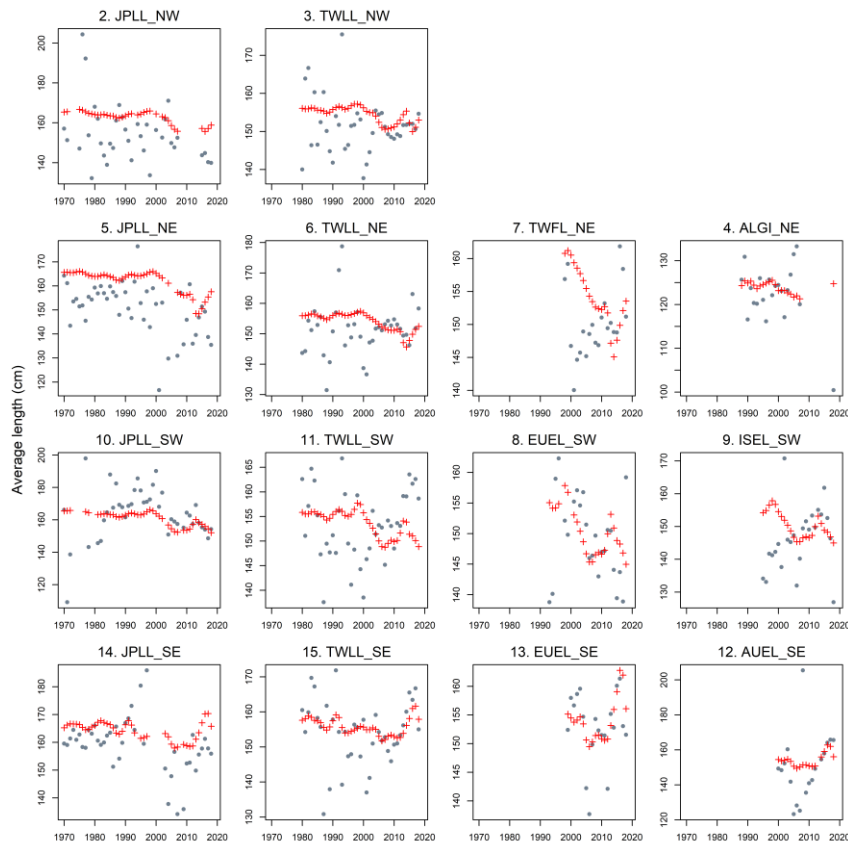

Figure 12: A comparison of the observed (grey points) and predicted (red points and line) average fish length (FL, cm) of swordfish by fishery for the basic model.

5.2.2 Model estimates

The estimated parameters in the basic model include: the overall population scale parameter *R0*, the time series of recruitment deviates, the distribution of recruitment among regions, the fishery selectivity parameters, the catchability parameters for the CPUE indices.

The length-specific selectivity functions are presented in Figure 13. The Japanese longline selectivity is attaining selectivity above 200 cm. The selectivity for the other longline fisheries (TWLL, EUEL) were estimated to be dome shaped, with peak selectivity occurring at about 150 – 200 cm. The doming effect of the Taiwanese longline selectivity is more pronounced, due to the lack of large fish in the catch samples (see Figure 5). The dome-shaped pattern may be consistent with the size/sex-based partitioning of the species, in which the largest, predominantly female individuals tend to be caught in the extremes of the range. The estimated selectivity for the ALGI fishery suggested the fish at 40–150 cm is most vulnerable to this fishery.

Recruitment deviates were estimated from 1970 – 2017 (Figure 14). There is a very strong signal suggesting that recruitment was very high immediately prior to the start of the targeted fishery in the 1990s, followed by anomalously low recruitment. This trend is suspicious, but without the recruitment anomalies, the model could not provide an adequate fit to the CPUE series. It was expected that the recruitment signal might be corroborated by the size data, but there was not a strong signal in mean sizes, except that the observed mean size for EUEL and AUEL fleet showed some decline through the 2000s (see **Error! Reference source not found.**)). The distribution of recruits showed very similar patterns among regions except for a large pulse in the NE preceding the anomalously large increase of the Japanese longline CPUE towards the end of the time series.

This basic model suggests that the population in the southern regions is considerably lower than the northern regions (Figure 15 – left). The most notable features are the increase in the population estimated around the early 1990s (the beginning of the targeted fishery), the general decline in all regions over the next 20 years. The more recent biomass trend to vary amongst regions, driven by the divergent regional CPUE. The SW region was estimated to be depleted the most, with current biomass estimated to be below 20% of the initial level , while current biomass in other regions were estimated to be above 40% of the unfished level (Figure 15 – right). Overall, the stock biomass appears to have been increasing since the mid-2000s, following the decline in the preceding decade (Figure 16).

The estimates of fishing mortality were relatively high for the Taiwanese fleets within NW and SW regions (Figure 17**Error! Reference source not found.**). In recent years, the EUEL fleet has the highest fishing mortality rates in the SW region. In the NW region, fishing mortality rates for the TWFL and ALGI fisheries have increased rapidly since the 1990s.
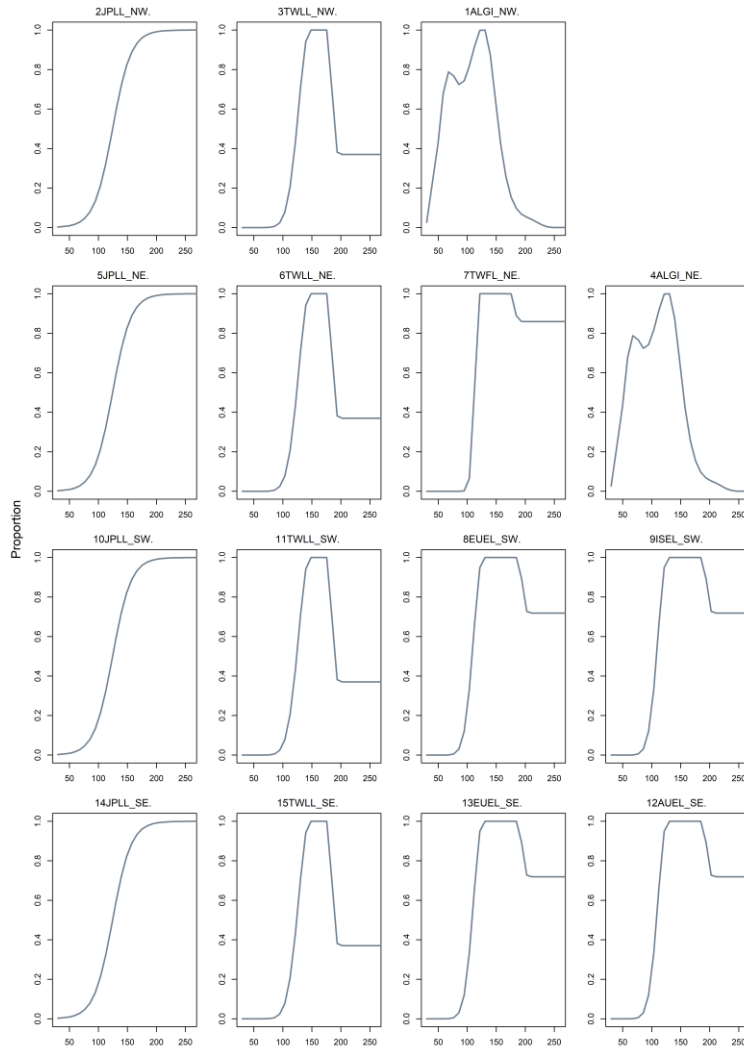
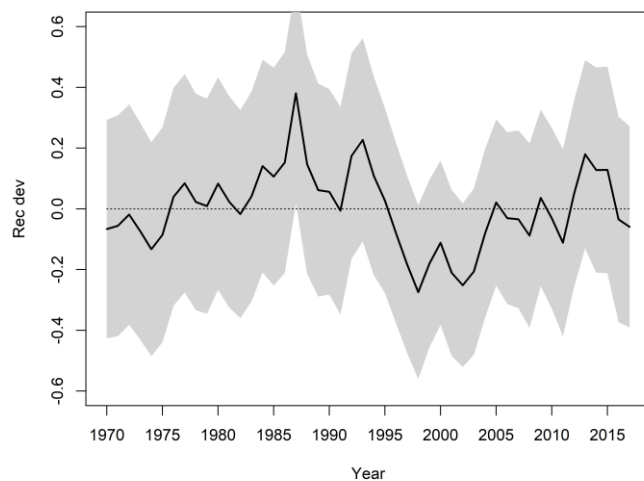**Figure 13: Length specific selectivity by fishery from the basic model.**

Figure 14: Recruitment deviates from the SRR with 95% confidence interval from the basic model
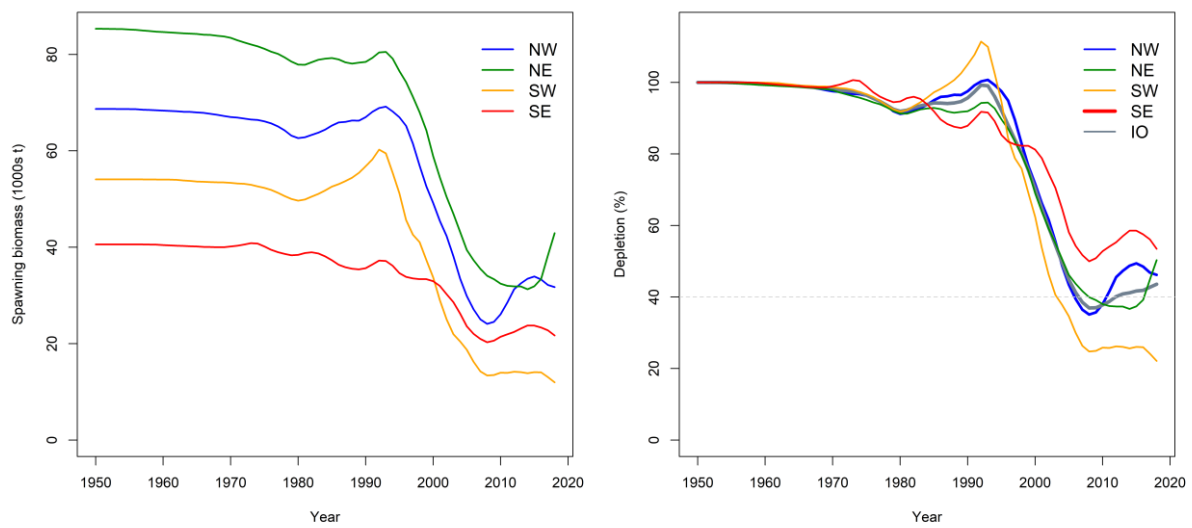
26

Figure 15: Estimated spawning biomass (left) and depletion (right) for the individual model regions from the basic model.
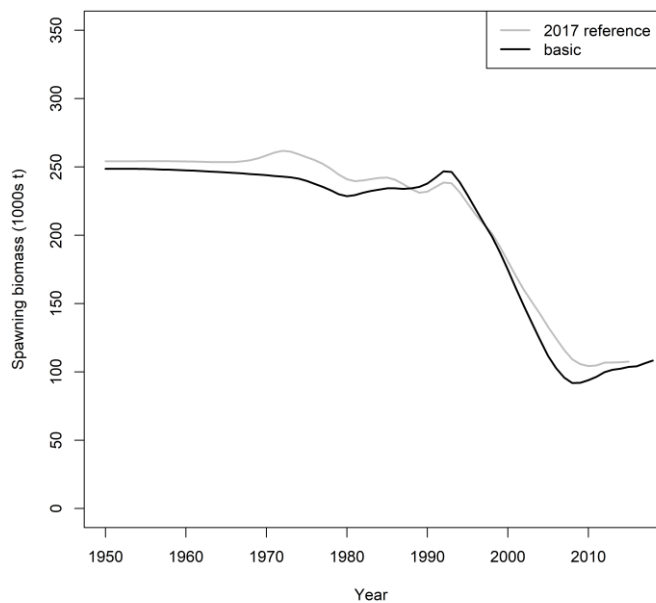

Figure 16: A comparison of estimated spawning biomass from the basic model and the 2017 reference model.
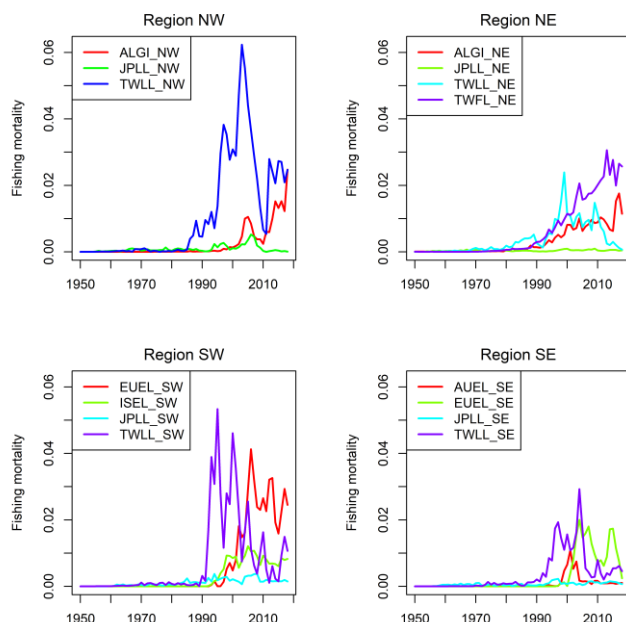
Figure 17: Trends in fishing mortality (annual) by fleet for the basic model

5.3 Sensitivity models

Selected results from the sensitivity models are provided in Appendix B. Table B1 summarised the estimates of key model quantities. The estimated SSB_0 ranged from 214105 to 504,255 t, MSY ranged from 28743 t to 61042 t, and current depletion ranged from 34% to 75%.

Sensitivity related to CPUE

The sensitivity models *cpueESP* and *cpueTWN* replaced the UPOR & UZAF indices in the SW region with the more optimistic UESP index, or the more pessimistic UTWLL index, respectively (Figure B2). The models yielded a biomass trend in the SW region which are reflective of the respective index (Figure B4). However, both models had a very minor effect on the overall SSB estimates in the IO (Figure B1).

The model *cpueIND* removed the UJPLL indices from 2011 in the NW and NE regions, and included UIND index (for NW) (Figure B2). This is to address that the recent UJPLL indices in the norther regions may not be as reliable due the low level of fishing effort. The model estimated lower stock biomass in IO for the recent years than the basic model (Figure B1).

Including the early JPLL indices (1979 – 1993) did not have any appreciable impact on model estimates (Figure B1). The catch during this period was relatively small and the CPUE appears to be noisy and uninformative of the depletion (Figure B2).

The UTWLL indices (4 regions) had a dramatic effect on the assessment model (Figure B1), with estimated SSB more than doubled that of the basic model. The result is not surprising – the UTWLL indices showed an a relatively flat trend in the northern regions through the 1990s to the 2000s when the catches are the highest, implying a high stock productivity. However, the reliability of the UTWLL indices during this period is questionable, given the rapid change of the fishery.

The basic model used a relatively small CV (0.1) for all CPUE indices, to ensure a reasonable fit to the CPUE (they are the only source of information on abundance). The use of a larger CV (0.2) did not have a large impact to model results but, the model was not able to adequately capture the extent of

decline in the CPUE in most regions. Consequently, the estimates of biomass trend are more optimistic (Figure B1).

Model *region* adopted the alternative regional scaling factors derived from the Japanese catch effort data (see Section 3.2.2). The new set of weighting factors implied that the least stock biomass of swordfish is residing in the SW region (Figure B4). The estimate of total biomass is very close to the basic model (Figure B1). The application of regional scaling factors in a spatially structure model significantly increases the power of the model to estimate the relative (and absolute) level of biomass among regions. The approach used was to determine regional scaling factors that incorporated both the size of the region and the relative catch rate is appropriate. Yet it is not known how well the aggregated Japanese catch effort data approximate the spatial density of swordfish, and further study is required to improve the estimates in order to reduce potential bias in the assessment model.

Sensitivity related to length composition data

The sample size for the length composition data was capped at 20 in the basis model. Further analysis showed that a larger sample size would lead to recruitment (and consequently biomass) mostly driven by the size data, which is not ideal given the considerable noise in the length composition data. The model with a smaller sample size (i.e. *CL005* where the sample size is capped at 5) estimated a noticeably lower level of biomass (Figure B1), without any appreciable deterioration in the fit to the length composition data or change in the estimates of selectivity. The sensitivity of biomass estimates to the sample size is reflective the conflict between the CPUE and length composition data and constitute an important source of uncertainty to the assessment model. As such both options on the sample size (5 and 20) were retained in the final model options.

Sensitivity related Biological parameters

The sensitivity models related to growth, recruit variability and steepness represent alternative, yet plausible values of the biological parameters of the stock. These alternative parameter values did not fundamentally change the conclusion of the assessment but constitute additional uncertainty to the model estimates (Figure B1).

There is no evidence in the data that can help differentiate the two growth options, although the likelihood from the fits to the length composition data slightly favours the growth estimates by Wang (2010). A larger σ_R resulted in larger recruitment variability but did not change the trend in estimated recruitment throughout the model period (Figure B5).

The steepness values appear to have little influence on the fits of data, but is very influential on estimates of MSY-related reference quantities. The stock-recruit function alone is not sufficient to explain the recruitment pattern, and the pattern of anomalous recruitment is similar regardless whether steepness is low or high. The h90 option seems to be at the higher end of results generally assumed for tuna stocks (ISSF 2011). Observations of other SWO populations which have experienced a decrease in fishing effort seem to show a rapid population rebound (North Atlantic, SW Pacific). Together with life history considerations, this suggests that the higher steepness values are probably likely for this species.

5.4 Final model options

The UJPLL, UPOR, and UZAF indices are a more credible set of abundance indices for IO swordfish (see Fu 2017, and the discussions in Sections 7), thus were included in the final model options. Other CPUE indices (UTWLL, UESP, and UIND) as alternative yet plausible scenarios were examined in sensitivity analysis and were down weighted in the final models to the extent that they had almost no influence on model estimates. The final model options also included three alternative values of steepness of the BH SRR (h 0.7, 0.8 and 0.9). These values are considered to encompass the plausible range of steepness values for swordfish

The final model ensemble corresponds to a full combination of three steepness values, two growth estimates, two levels of recruitment variability, and two levels of weighting on the length composition data, with a total of 24 models (see Table 6). These models encompass a wide range of stock trajectories (Figure 18). Across the model grid, initial spawning biomass (SSB0) ranged from 202,280 to 312,127t, current depletion ranged from 35% to 48% (SSB2018/SSB0) (Table 7). In general, higher stock biomass are associated with higher weighting of length composition data, and higher recruitment variability, and a lower steepness value (2010).
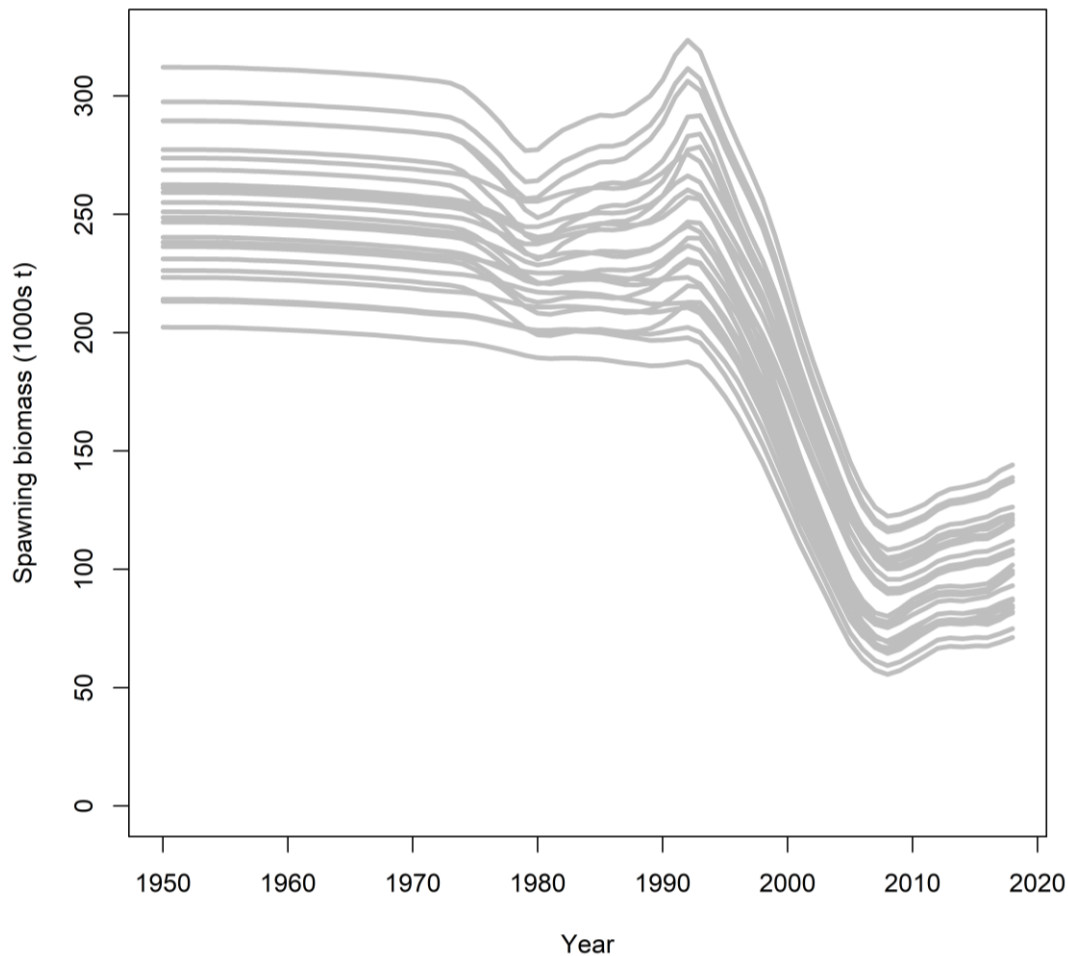
Figure 18: Spawning biomass trajectories from the final model grid (details in Table 5: Description of the sensitivity models for the 2020 assessment. Changes are relative to the basic model.

Model	Description
CPUE indices	
cpueESP	The UPOR and UZAF in the SW region replaced by the UESP 2001 – 2018
cpueTWN	The UPOR and UZAF in the SW region replaced by the UTWLL 2000 – 2018;
cpueIND	Removed UJPLL 2011– 2018 in NW and NE regions; included the UIND 2006 – 2018 in the NE region.
cpuePre	Included the UJPLL-pre (1979-1993) for all regions.
TWP	Removed all UJPLL; included UTWLL 1994 – 2018 for NW, NE, and SE; included UTWLL 1994 – 2003, UPOR 2000 – 2018, and UZAF 2004 – 2018 for SW; shared Taiwanese regional catchability coefficient.
cv20	A CV of 0.2 for all indices
region	Alternative CPUE regional scaling factors developed from catch effort data
Length composition	
CL005	Down weighting the length composition data with the sample sizes reduced to a maximum of 5.
Biological parameters	
GtMf	Growth estimates from Wang et al. (2010)
r4	Recruitment deviation $\sigma_R = 0.4$.
h70	Recruitment steepness = 0.7
h90	Recruitment steepness = 0.9

5.5 Final model assessable (grid)

On basis of the exploratory analysis, final options were configured to capture the uncertainty related to assumptions on the stock-recruitment steepness, recruitment deviations, growth, and effective sample sizes on the length composition data, which are thought to contribute to the main sources of uncertainty (Table 6). Thus, the final models involved running a full combination of options on steepness (3 values), σ_R (2 values), growth (2 options), and length composition data sample size (2 values), with a total of 24 models.

Table 6).

Table 7: Estimates of management quantities for the stock assessment model options. Current yield (mt) represents yield in 2018 corresponding to fishing mortality at the FMSY level.

Option	SB_0	SB_{MSY}	SB_{MSY}/SB_0	SB_{2018}	SB_{2018}/SB_0	SB_{2018}/SB_{MSY}	F_{2018}/F_{MSY}	MSY
io4_h70_GtMf_r2_CL020	273,771	76,220	0.28	126,360	0.46	1.66	0.65	31,676
io4_h70_GtMf_r2_CL005	238,194	66,642	0.28	93,162	0.39	1.40	0.83	27,825
io4_h70_GtMf_r4_CL020	312,127	86,995	0.28	144,087	0.46	1.66	0.59	35,806
io4_h70_GtMf_r4_CL005	259,220	72,643	0.28	101,837	0.39	1.40	0.79	30,066
io4_h70_GoMf_r2_CL020	261,159	72,464	0.28	111,975	0.43	1.55	0.71	30,019
io4_h70_GoMf_r2_CL005	231,165	64,248	0.28	81,555	0.35	1.27	0.90	26,899
io4_h70_GoMf_r4_CL020	289,535	80,409	0.28	123,114	0.43	1.53	0.66	33,074
io4_h70_GoMf_r4_CL005	251,015	69,906	0.28	86,872	0.35	1.24	0.85	29,023
io4_h80_GtMf_r2_CL020	262,497	62,035	0.24	123,160	0.47	1.99	0.53	34,987
io4_h80_GtMf_r2_CL005	223,300	53,094	0.24	87,568	0.39	1.65	0.69	30,038
io4_h80_GtMf_r4_CL020	297,524	70,354	0.24	138,786	0.47	1.97	0.48	39,407
io4_h80_GtMf_r4_CL005	246,709	58,819	0.24	99,323	0.40	1.69	0.64	32,910
io4_h80_GoMf_r2_CL020*	248,650	58,607	0.24	108,315	0.44	1.85	0.58	32,951
io4_h80_GoMf_r2_CL005	214,105	50,586	0.24	74,921	0.35	1.48	0.76	28,743
io4_h80_GoMf_r4_CL020	277,337	65,465	0.24	120,497	0.43	1.84	0.53	36,497
io4_h80_GoMf_r4_CL005	236,348	56,013	0.24	83,672	0.35	1.49	0.70	31,478
io4_h90_GtMf_r2_CL020	255,017	47,059	0.18	121,647	0.48	2.58	0.41	38,947
io4_h90_GtMf_r2_CL005	213,245	39,629	0.19	84,628	0.40	2.14	0.54	32,844
io4_h90_GtMf_r4_CL020	289,436	53,490	0.18	137,199	0.47	2.56	0.37	43,914
io4_h90_GtMf_r4_CL005	238,097	44,477	0.19	98,053	0.41	2.20	0.49	36,326
io4_h90_GoMf_r2_CL020	240,329	44,396	0.18	106,553	0.44	2.40	0.44	36,506
io4_h90_GoMf_r2_CL005	202,280	37,500	0.19	71,217	0.35	1.90	0.60	31,133
io4_h90_GoMf_r4_CL020	268,780	49,792	0.19	118,922	0.44	2.39	0.41	40,521
io4_h90_GoMf_r4_CL005	226,240	42,167	0.19	82,052	0.36	1.95	0.54	34,497

* basic model

33

5.6 Diagnostics

Several diagnostic tools were run for the basic model, including likelihood profiling, ASPM analysis, and retrospective analysis.

5.6.1 Profile likelihood

The likelihood profile on the population scaling parameter (R0) did not show major conflicts between datasets (Figure 19). Overall, the CPUE and size data appeared to have provided information on both the upper and lower bounds for the stock abundance, although the CPUE data favour a relatively smaller R0 whereas the size data imply a larger R0. The total likelihood is also strongly driven by the recruitment penalty function which penalises large recruit anomalies (required to support the catch history for a small R0. An additional jittering analysis suggested the model has attained the minimum in the likelihood surface examined.
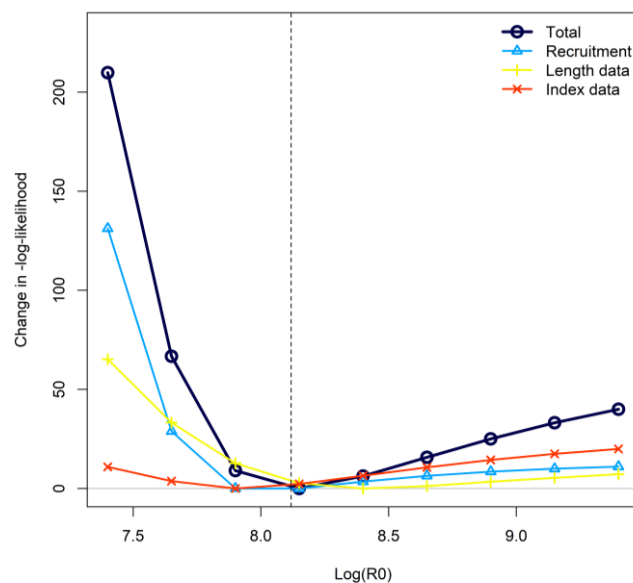

Figure 19:Likelihood profile including total and component likelihood function values for the basic model.

5.6.2 ASPM analysis

The Age Structured Production Model (ASPM) analysis (Maunder & Piner 2015) was used to illustrate what is the main driver of the population trend, and whether the composition data has an undue influence on the estimates of abundance. The ASPM analysis involved running a variation of the basic model: where the length composition data were removed from the model (selectivity parameters fixed at the estimates from the basic model) and recruitment deviates were fixed to be zero.

The stock biomass from the ASPM model is shown in Figure 20. The analysis indicated that there is high degree of consistency between the catches and abundance indices for the swordfish stock, i.e. the catch alone explains reasonably well the historical abundance trend concerning the major decline, although a declining recruitment is also required in order to fully accommodate level of deletion for 1990 – 2010. The ASPM analysis further corroborated the profile likelihood on the influence of the length composition data on estimates of the overall stock abundance.
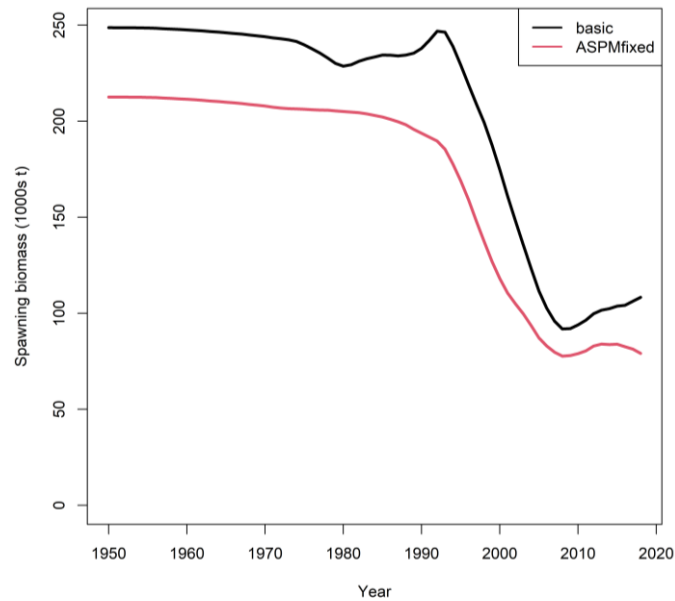
Figure 20: SSB estimates from the ASPM analysis.

5.6.3 Retrospective analysis

Retrospective analysis is diagnostic approach to reveal systematic bias in the model estimation. It involves fitting a stock assessment model to the full dataset. The same model is then fitted to truncated datasets where the data for the most recent years are sequentially removed. The retrospective analysis was conducted to the basic model for the last 5 years of the assessment to evaluate whether there were any strong changes in model results. The analysis indicated there is negligible retrospective pattern for key parameter and reference points estimates, which provided some confidence on the robustness of the model with respect to the inclusion of recent observational data.
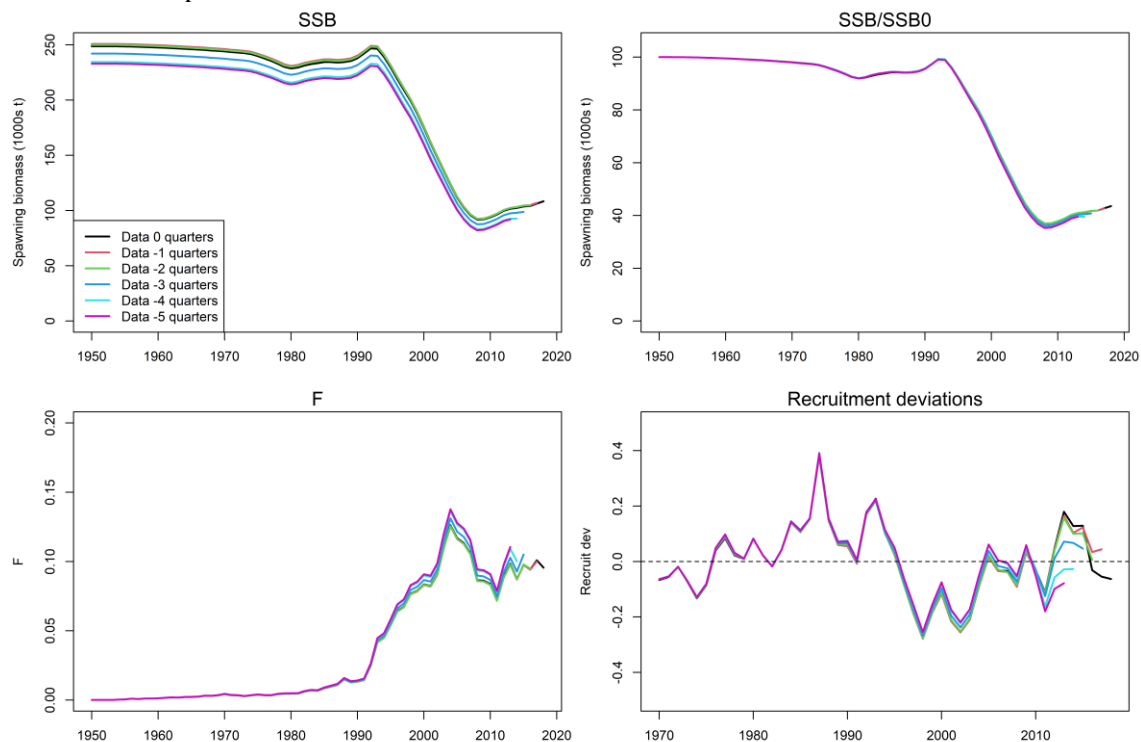

Figure 21: Retrospective analysis summary for the basic model.

35

6. STOCK STATUS

6.1 Current status and yields

MSY based estimates of stock status were determined for the final model options, including alternative assumptions on growth, alternative values of SRR steepness and recruitment variability, and the alternative weighting of length composition data. Stock status was determined for individual models (Table 7), as well as the for all (24) models combined, incorporating uncertainty of each model based on estimated variance-covariance matrix of parameters (Table 8).

MSY based reference points were derived based on the average F-at-age matrix in 2018, representing the most recent pattern of exploitation from the fishery. For the selected model options, point estimates of *MSY* ranged from 26, 900 t to 43 914 t (Table 7). Models with higher steepness generally yielded comparatively higher estimates of *MSY*. Annual catches since the 1990s have been within the range of the estimated MSY (Figure 22).

In general, current stock biomass relative to the *MSY* based benchmarks are not fundamentally different for the range of model options, although the proximity to the *MSY* benchmarks is sensitive to the different of assumptions. Averaging across the model grid, fishing mortality rates have been increasing since 1990s, and then decreased after the 2000s. Fishing mortality rates have remained relatively stable since 2010 and are well below the F_{MSY} (Figure 22). Biomass was estimated to have declined considerably from the 1990s through to the 2000s and have slightly increased since 2010 (Figure 22).

Estimates were combined across from the 24 models to generate the final KOBE stock status plot (Figure 23). For individual models, the uncertainty is characterised using the multivariate lognormal Monte-Carlo approach (Walter et al. 2019, Walter & Winker 2019, Winter et al. 2019), based on the maximum likelihood estimates and variance-covariance of F/F_{MSY} and SSB/SSB_{MSY}. Thus, estimates of final stock status included both within and across model uncertainty. Combined across the model ensemble, SSB_{2018} was estimated to be of 1.71 SSB_{MSY} (1.20– 2.22), and F_{2018} was estimated 0.60 F_{MSY} (0.41–0.85) (Table 8). The probability of the stock being in the green Kobe quadrant in 2018 is estimated to be over 95%. The stock is therefore considered not to be overfished and is not subject to overfishing in 2018.

Table 8: Estimated Status of swordfish in the Indian Ocean from the final model grid (Median and 80% quantile range).

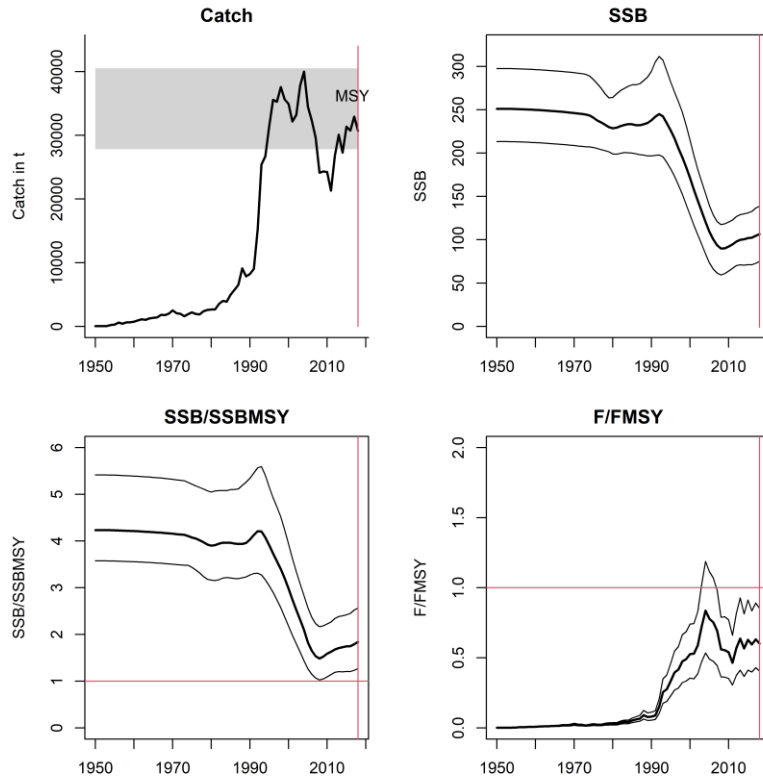|	
Catch in 2018:	30 600
Average catch 2014–2018:	30 686
MSY (1000 t) (80% CI):	33 (27 –40)
F_{MSY}	0.23 (0.15–0.31)
SB_0(1000 t) (80% CI):	250 (210–295)
SB_{2018} (1000 t) (80% CI):	102 (70–138)
SB_{MSY}	59 (41–77)
SB_{2018}/SB_0 (80% CI):	0.42 (0.36–0.47)
SB_{2018}/ SSB_{MSY}	1.75 (1.28–2.35)
F_{2018}/ F_{MSY}	0.60 (0.40–0.83)

Figure 22: Estimated stock trajectories for the Indian Ocean swordfish from the final model grid. Thin black lines represent 5%, 50%, 95% percentiles. In the catch plot, dotted lines represent estimate of MSY, the shaded area represents 5th and 95th percentiles
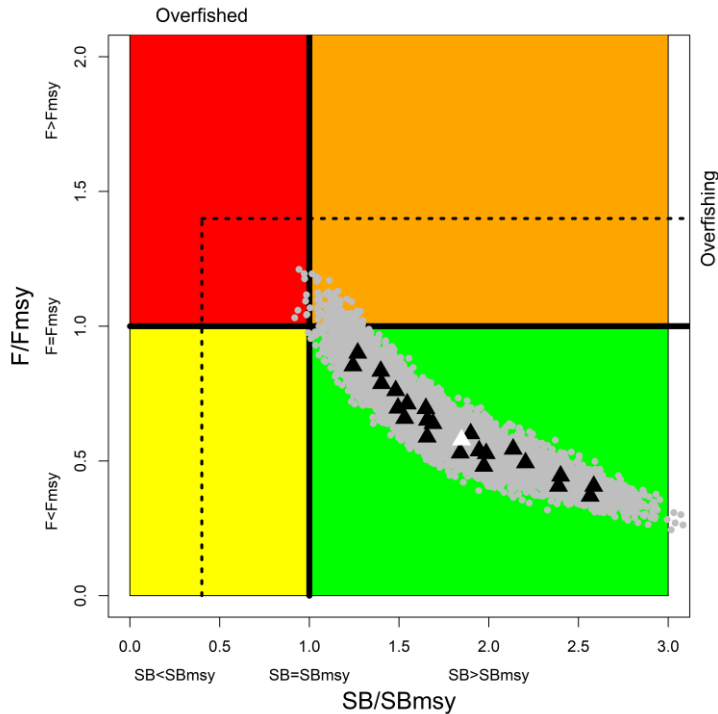

Figure 23: current stock status, relative to SB_{MSY} (x-axis) and F_{MSY} (y-axis) reference points for the final model grid. Triangles represent MPD estimates from individual models (white triangle represent the estimate from the basic model). Grey dots represent uncertainty from individual models. The dashed lines represent limit reference points for IO swordfish ($SB_{lim} = 0.4$ SB_{MSY} and $F_{lim} = 1.4$ F_{MSY}).

6.2 Projection

Stock projections were conducted for the final model grid. For each model, the projections were conducted for a 10-year period (2019–2028) at a constant level of catch set as a multiple of the fishery catches in 2018. Five levels of catch were investigated representing 60% to 140% (in incremental of 20%) of the 2018 catch level. Recruitment during the projection period was at the equilibrium level. For each catch scenario, the probability of the biomass being below the SB_{MSY} level and the probability of fishing mortality being above F_{MSY} were determined over the projection horizon (2019 – 2028) using the delta-MVLN estimator (Walter & Winker 2019), based on the variance-covariance derived from estimates of SB/SB_{MSY} and F/F_{MSY} across the model grid. Thus, the estimator incorporated only the structure uncertainty across the final model options, which is thought to be much larger than the within model uncertainty of individual models.

Under the current levels of catches, the stock biomass is projected to remain relatively stable, with a high probability of maintaining at or above the SB_{MSY} for the longer term. An increase of 40% or more from current catch levels will likely result in the biomass being dropping below the SB_{MSY} level for the longer term (with close to 50% probability).

Table 9: Projected stock status: the probability of spawning biomass being below SB_{MSY} and fishing mortality being above F_{MSY} for 2019 – 2028 for five alternative levels of catch relative to 2018 (93 515 mt) for final model grid.

										Pr (B<Bmsy)
Catch	2019	2020	2021	2022	2023	2024	2025	2026	2027	2028
60%	0.00	0.00	0.00	0.00	0.00	0.00	0.00	0.00	0.00	0.00
80%	0.00	0.00	0.00	0.00	0.00	0.00	0.00	0.00	0.00	0.00
100%	0.00	0.00	0.00	0.01	0.01	0.01	0.01	0.02	0.02	0.02
120%	0.00	0.00	0.01	0.02	0.03	0.06	0.08	0.11	0.13	0.18
140%	0.00	0.01	0.01	0.04	0.10	0.17	0.25	0.32	0.40	0.47

										Pr (F>Fmsy)
Catch	2019	2020	2021	2022	2023	2024	2025	2026	2027	2028
60%	0.00	0.00	0.00	0.00	0.00	0.00	0.00	0.00	0.00	0.00
80%	0.00	0.00	0.00	0.00	0.00	0.00	0.00	0.00	0.00	0.00
100%	0.02	0.03	0.04	0.04	0.04	0.05	0.06	0.07	0.06	0.07
120%	0.10	0.13	0.18	0.21	0.26	0.30	0.32	0.35	0.38	0.42
140%	0.25	0.34	0.44	0.51	0.57	0.62	0.66	0.70	0.73	0.78

7. DISCUSSION

This report presents a preliminary stock assessment for Indian Ocean swordfish using a spatially disaggregated, sex-explicit, and age-structured model. It represents an update and revision of the 2017 assessment model with newly available information, including updated reginal longline CPUE indices and length composition data. There are no fundamental changes in the structure of the assessment model compared to the previous assessment (Fu 2017), with the revisions mostly concerning the adoption of a revised fleet structure to account for potential difference in fishery selectivities. A basic model was configured to assess the model performance and diagnostics. A range of sensitivity models were explored to assess the impact of key data sets and model assumptions. The final model options involved running a combination of parameter and assumption options related to the stock-recruitment steepness, recruitment variability, growth, and weighting on the length composition data. The final estimates of stock status are based on a model grid of 24 models, incorporated uncertainty estimates from both within and across the model ensemble.

The overall stock status estimates obtained from the range of model options do not differ substantially from the previous assessment. Considering the quantified uncertainty, spawning stock biomass in 2018 was estimated to be 42% of the unfished levels and 170% of the level that can support MSY (SSB2018/SSBMSY = 1.75). With high likelihood, current fishing mortality was estimated to be lower than FMSY (F2018/FMSY = 0.6). The stock is considered not to be overfished and is not subject to overfishing in 2018. The retrospective analysis provided some confidence on the robustness of the model with respect to recent data, yet the uncertainly on levels of most recent recruitment may undermine the predictive capabilities of the model. Annual catches since the 1990s have been within the range of the estimated MSY and the current catch level is projected to be sustainable over the longer term.

The Indian Ocean swordfish fisheries present a number of unique problems in the development of a stock population model: there is a lack of good information on recruitment; there is considerable uncertainty on growth, maturity, and natural mortality; there are good time series of CPUE, but their reliability to track abundance is highly uncertain, given the conflicts between these time series; there is also a large amount of data on size structure, but the sampling may be not random. As with earlier assessments, the models presented here, while fairly representing some of the data (e.g., the biomass indices), also show some signs of poor fit. The assessment tested various combinations of assumptions to explore the sensitivity and describe the uncertainty in the stock status. It is unlikely the estimates of historical stock size are accurate, given assumptions about annual recruitment and the reliance on the historical catch-effort indices of abundance. Current stock status as estimated here should thus be treated with caution.

The Japanese and Taiwanese longline fleets have traditionally been used to generate the abundance indices for Indian Ocean swordfish stocks. These fleets have an extensive history, broad spatial coverage, and substantive logbook programmes. However, the operations of these fleets have changed historically, with large shifts in targeting that are poorly quantified. Conventional fisheries theory suggests that the depletion estimated by the Japanese series has been more consistent with the swordfish exploitation history than the Taiwanese series, and this interpretation has generally been given more weight in the assessment and management advice (Kolody 2011). It is widely known that the catch efficiency of swordifih has experienced dramatic changes in the late 1980s and early 1990s with the deveopment of fresh-chill longline fleets which have further improved on catch rates through refinements to fishing gear such as the the introduction of light sticks and monofilament longlines in this period (Ward & Elscot 2000).

The abrupt decline in the JPN CPUE in the 1990s is the strongest signal in the assessment that drives the inference of very high depletion in most regions. The drop is so steep that the assessment models can only explain it through a combination of fishery depletion and anomalous recruitment (Martell 2010, Kolody 2010). However, it is recognized that the Japanese fleet underwent some changes in the 1990s

that might be exaggerating the estimated level of swordfish depletion at that time (Kolody 2011). The recent trend in the Japanese CPUE in the northern regions is also suspicious: the very large increase in the index coincided with the period when vessels returned to the old fishing ground that had been avoided for several years due to the threat of piracy. The increase may be related to a combination of factors including increase in abundance and major changes in catchability, implying a possible non-linear relationship between CPUE and abundance.

The conflicts amongst CPUE indices in the SW region represent a concern, because there is a perception that this region may be excessively depleted. The recent Japanese CPUE is increasing, while the Portugal and South African CPUE are decreasing and Taiwanese CPUE is steeply decreasing. In contrast, the CPUE from Spain are relatively stable. The effort from the Taiwanese fleet since 2005 in the region is very low, and this casts doubt on the reliability of the apparent population collapse. We would tend to trust the Portuguese and South African series more than the others because: (i) the indices are based on a swordfish target fishery; (ii) these fleets seem to have operated consistently over the recent time period, and ii) the standardisation analyses were very robust to different assumptions.

The assessment is assuming a single IO stock disaggregated into 4 areas with shared spawning and foraging grounds site fidelity. There are very few direct observations of swordfish migration in the Indian Ocean. The few conventional tag recaptures and satellite GPS tag deployments near the Australian coast provided no indication of large-scale movements, but these studies are limited by biased recovery effort and short deployment times respectively (Karen Evans, CSIRO, Australia, pers. comm.). Tagging studies from other oceans suggested residency or homing behaviour amongst components of populations (Carey and Robinson 1981), although a few trans-Atlantic swordfish migrations have been recorded (Kadagi et al 2011). However, it can be indirectly inferred that there are probably some relatively large seasonal migrations. Swordfish can be caught at least as far south as 45° S, however, the spawning regions (and larval distributions) have all been identified in the tropical regions. In the southern hemisphere at least, this suggests substantial directed seasonal migrations. The spawning season also seems to be several months out of phase between the northern and southern regions. It is not clear whether this represents a single annual migration between north and south, or whether distinct populations independently move between lower and higher latitudes in each hemisphere. However, in many cases, resolving the directed seasonal migration patterns is not required in an assessment.

8. ACKNOWLEDGMENTS

9. REFERENCES

Anon. 2006. Report of the Fifth session of the IOTC working party on billfish. Colombo, Sri Lanka, 27-31 MAR 2006.

Bourjea, J., Le Couls S., Grewe P., Evano H. and Muths D. 2011. Preliminary results of the Indian Ocean swordfish stock structure project – IOSSS – focus on the population genetic approach. IOTC-2011-WPB-09-info-5.

Bradman, H., Grewe, P. and Appleton, B. 2010. Direct comparison of mitochondrial markers for the analysis of swordfish population structure. Fisheries Research 109: 95–99.

Campbell, R. 1998. Longline effort in the eastern AFZ. Unpublished paper presented at the Eastern

Tuna and Billfish Fishery Effort Setting Workshop, Canberra, 20 November 1998.

Carey, F.G., Robinson, B.H. 1981. Daily patterns in the activities of swordfish, Xiphias gladius, observed by acoustic telemetry. Fisheries Bulletin 79(2), pp.277-292.

Davies, N., Pilling, G., Harley, S., Hampton, J. 2013. Stock assessment of swordfish (*Xiphias gladius*) in the southwest Pacific Ocean. WCPFC-SC9-2013/SA-WP-05.

Cartelle, A.R., Costa, F.J., A., Mejuto, J. 2020. Updated Standardized Catch Rates of Swordfish (*Xiphias Gladius*) Caught by the Spanish Surface Longline Fleet in the Indian Ocean During the 2001-2018 Period. IOTC–2020–WPB18–12.

Farley, J., Clear, Naomi., Kolody, D., Krusic-Golub, K,. Eveson, Paige., Young, Jock. 2016. Determination of swordfish growth and maturity relevant to the southwest Pacific stock. R 2014/0821.

Francis, R.I.C.C. 2012. Data weighting in statistical fisheries stock assessment models. Canadian Journal of Fisheries and Aquatic Sciences, 2011, 68(6): 1124-1138.

Geehan, J. 2018. Revision to the IOTC scientific estimates of Indonesia's fresh longline catches. IOTC-2018-WPDCS14-23.

Geehan, J, Seyyadji, B. 2018. Revision to the IOTC Scientific Estimates of Indonesia's Fresh Longline Catches. IOTC-2018-WPB16-22

Hoyle, S., Langley, A. 2007. REGIONAL WEIGHTING FACTORS FOR YELLOWFIN TUNA IN WCP-CA STOCK ASSESSMENTS. WCPFC-SC3-ME SWG/WP-1.

Hoyle, S., Langley, A. 2020. Scaling factors for multi-region stock assessments, with an application to Indian Ocean tropical tunas/ Fisheries Research. 10.1016/j.fishres.2020.105586.

IOTC Secretariat. 2004. Disaggregation of Catches Recorded Under Aggregates of Gear and Species in the IOTC Nominal Catches Database. IOTC-2004-WPTT-06.

IOTC–WPB15. 2017. Report of the 15thSession of the IOTC Working Party on Billfish. San Sebastian, Spain, 2017. IOTC–2017–WPB15–R[E]: 106 pp.
ISSF 2011. Report of the 2011 ISSF stock assessment workshop, Rome, Italy, March 14-17. Unpublished report. 18pp.

IOTC Secretariat. 2020. Review of the Statistical Data and Fishery Trends for Billfish. IOTC–2019–WPB17–07.

Kadagi, N.I., Harris, T., and Conway, N. 2011. East Africa billfish Conservation and Research: Marlin, Sailfish and Swordfish Mark-Recapture field studies. IOTC-2011-WPB09-10.

Kolody, D. 2009. Exploratory Modelling of the Indian Ocean Swordfish Fishery, using an age-structured, sex-structured and spatially-disaggregated implementation of Stock Synthesis software.

Kolody, D. 2010. A Spatially-Structured Stock Synthesis Assessment of the Indian Ocean Swordfish Fishery 1950-2008, including Special Emphasis on the SW Region. Working paper for the IOTC Billfish Working Party July 2010: IOTC-2010-WPB-05.

Kolody, D. 2011. Review of CPUE Issues for the 2011 Indian Ocean Swordfish Stock Assessment. IOTC-2011-WPB09-13.

Kolody, D., R. Campbell, and N. Davies. 2008. A MULTIFAN-CL stock assessment of south-Pacific swordfish 1952-2007, WCPFC-SC4-2008/SA-WP-6 (Revision 1).

Kolody, D.; Herrera, M. 2011. An Age-, Sex- and Spatially-Structured Stock Assessment of the Indian Ocean Swordfish Fishery 1950-2009, including Special Emphasis on the South-West Region. OTC-2011-WPB-17.

Langley, A. 2016. Stock assessment of bigeye tuna in the Indian Ocean for 2016 — model development and evaluation. IOTC-2016-WPTT18-20.

Lu, C,P., Chen, C.A., Hui, C.F., Tzeng, T.D., Yeh, S.Y. 2006. Population genetic structure of the swordfish, *Xiphias gladius* (Linnaeus 1758), in the Indian Ocean and West Pacific inferred from the complete DNA sequence of the mitochondrial control region. Zoological studies 45(2): 269-279.

Martell, S. 2010. SCAM Swordfish Stock Assessment. Working Party IOTC-2010-WPB-14.

Methot Jr, R.D., Wetzel, C.R. 2013. Stock synthesis: A biological and statistical framework for fish stock assessment and fishery management. Fisheries Research, 142(0): 86-99.

Methot Jr, R.D., Taylor, I.G., Doering, K. 2020. 2020. Stock Synthesis User Manual Version 3.30.15. U.S. Department of Commerce, NOAA Processed Report NMFS-NWFSC-PR-2020-05.

Nishikawa, Y., Honma, M., Ueyanagi, S., Kikawa, S. 1985. Average distribution of larvae of oceanic species of scombrid fishes, 1956–1981. Far Seas Fisheries Research Laboratory, Shimizu. S Series 12. WPTT-04-06.

Nishida, T. 2008. Notes on the standardized swordfish CPUE of tuna longline fisheries (Japan and Taiwan) in WPB6 (1980-2006 and 1992-2006). IOTC-2008-WPB-INF04.

Parker, D., Kerwath, S.E. Standardized Catch per Unit Effort of Swordfish (*Xiphias Gladius*) for the South African Longline Fishery. IOTC–2020–WPB18–13

Penny, A.J., Griffiths, M.H. 1998. A first description of the developing South African pelagic longline fishery. Working paper SCRS/98 presented at the SCRS Swordfish Working Meeting. ICCAT, Mardrid.

Punt, A. E., Dorn, M.W., and Haltuch, M.A. 2008. Evaluation of threshold management strategies for groundfish off the USWest Coast. Fisheries Research, 94: 251–266.

Punt, A. E., Smith, A. D. M., Smith, D. C., Tuck, G. N., and Klaer, N. L. 2014. Selecting relative abundance proxies for BMSY and BMEY. – ICES Journal of Marine Science, 71: 469–483.

Setyadji, B., Parker, D., Wang, S.P. Fahmi, Z. 2020. Standardized CPUE of swordfish (*Xiphias Gladius*) from Indonesian tuna longline fleets in the north-eastern Indian Ocean. IOTC–2020–WPB18–20.

Sharma, R., Herrera, M. 2016. An Age-, Sex- and Spatially-Structured Stock Assessment of the Indian Ocean Swordfish Fishery 1950-2012, USING STOCK SYNTHESIS. IOTC–2014–WPB12–26_Rev2.

Taki, K., Ijima, H., Semba.Y. 2020. Japanese Longline CPUE Standardization (1979-2018) for Swordfish (Xiphias gladius) in the Indian Ocean using zero-inflated Bayesian hierarchical spatial model. IOTC–2020–WPB18–12.

Ward, P., Elscot, S. 2000. Broadbill swordfish: Status of world fisheries: Bureau of Rural Sciences, Canberra.
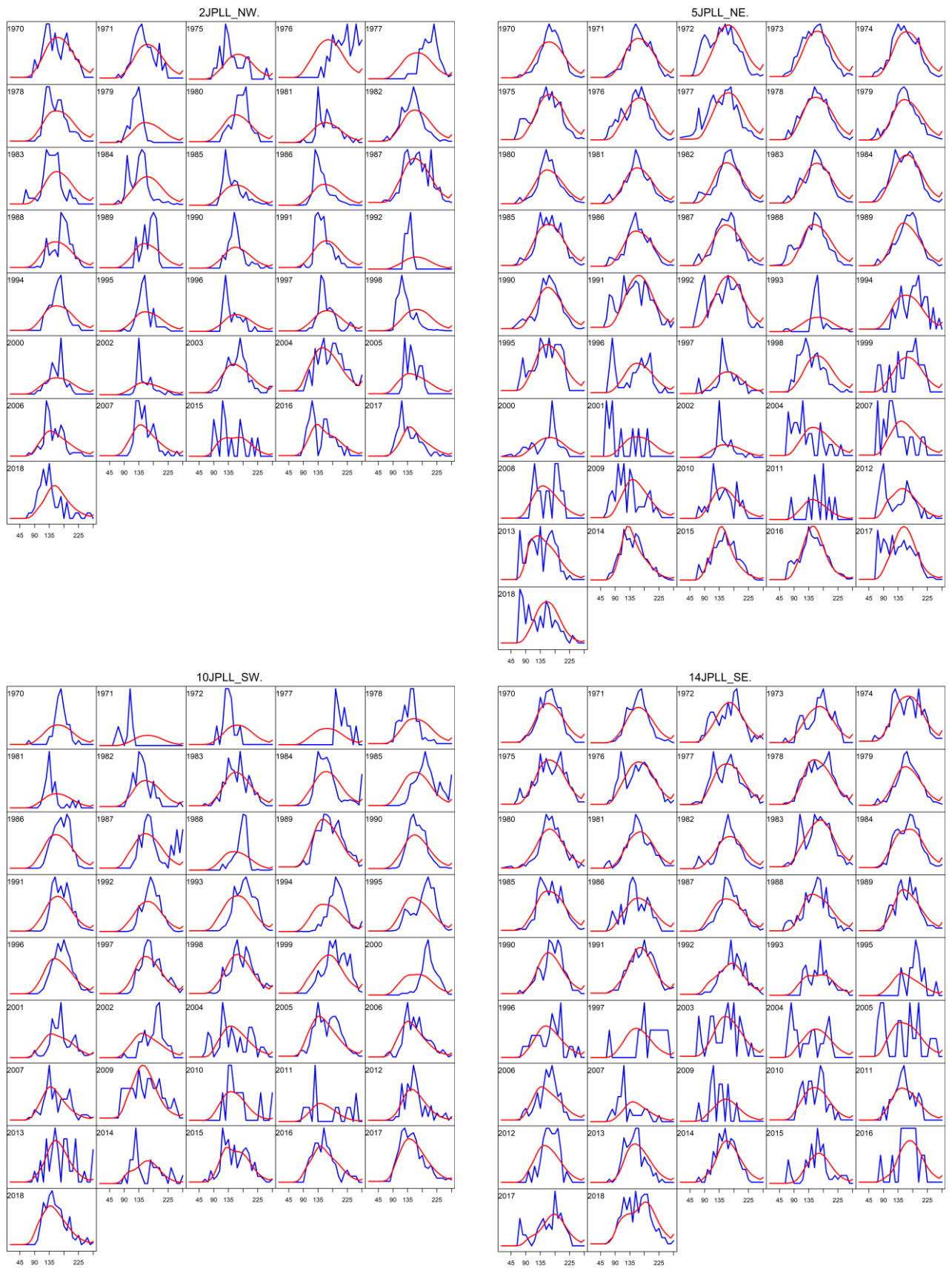
Wang, S.P. 2020. CPUE Standardization of Swordfish (*Xiphias gladius*) Caught by Taiwanese Large Scale Longline Fishery in the Indian Ocean. IOTC–2020–WPB18–15.

Wang, S.P., Chi-Hong, L., Chiang, W.C. 2010. Age and growth analysis of swordfish (Xiphias gladius) in the Indian Ocean based on the specimens collected by Taiwanese observer program. Working paper IOTC-2010-WPB-08 (revision 1).

Young, J. and A. Drake. 2002. Reproductive dynamics of broadbill swordfish (Xiphius gladius) in the domestic longline fishery off eastern Australia. Final report for project 1999/108, Fisheries Research Development Corporation, Canberra, Australia.

Young, J., Drake, A. 2004. Age and growth of broadbill swordfish (Xiphius gladius)from Australian waters. Final report for project 2001/014, Fisheries Research Development Corporation, Canberra, Australia.

Young, J., Humphreys, R., Uchiyama, J., Clear, N. 2008. Comparison of swordfish maturity and ageing from Hawaiian and Australian waters. WCPFC-SC3-BI SWG/WP-1.

APPENDIX A: FITS TO LENGTH DATA FOR MAIN FLEETS FROM THE BASIC MODEL

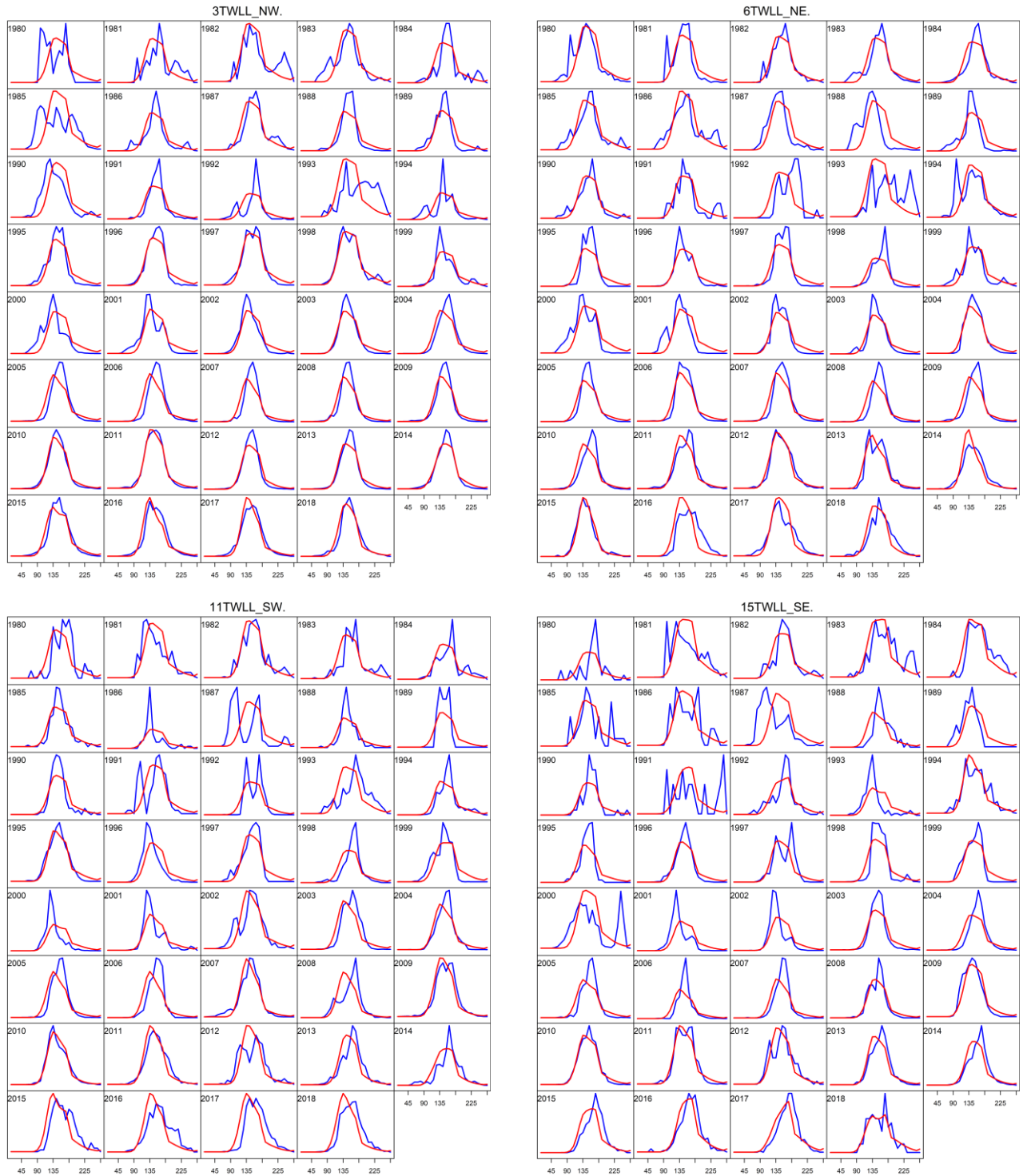**Figure A1. Observed (blue) and predicted (red) length compositions for the four Japanese longline fisheries.**

Figure A2. Observed (blue) and predicted (red) length compositions for the four Taiwanese fisheries.
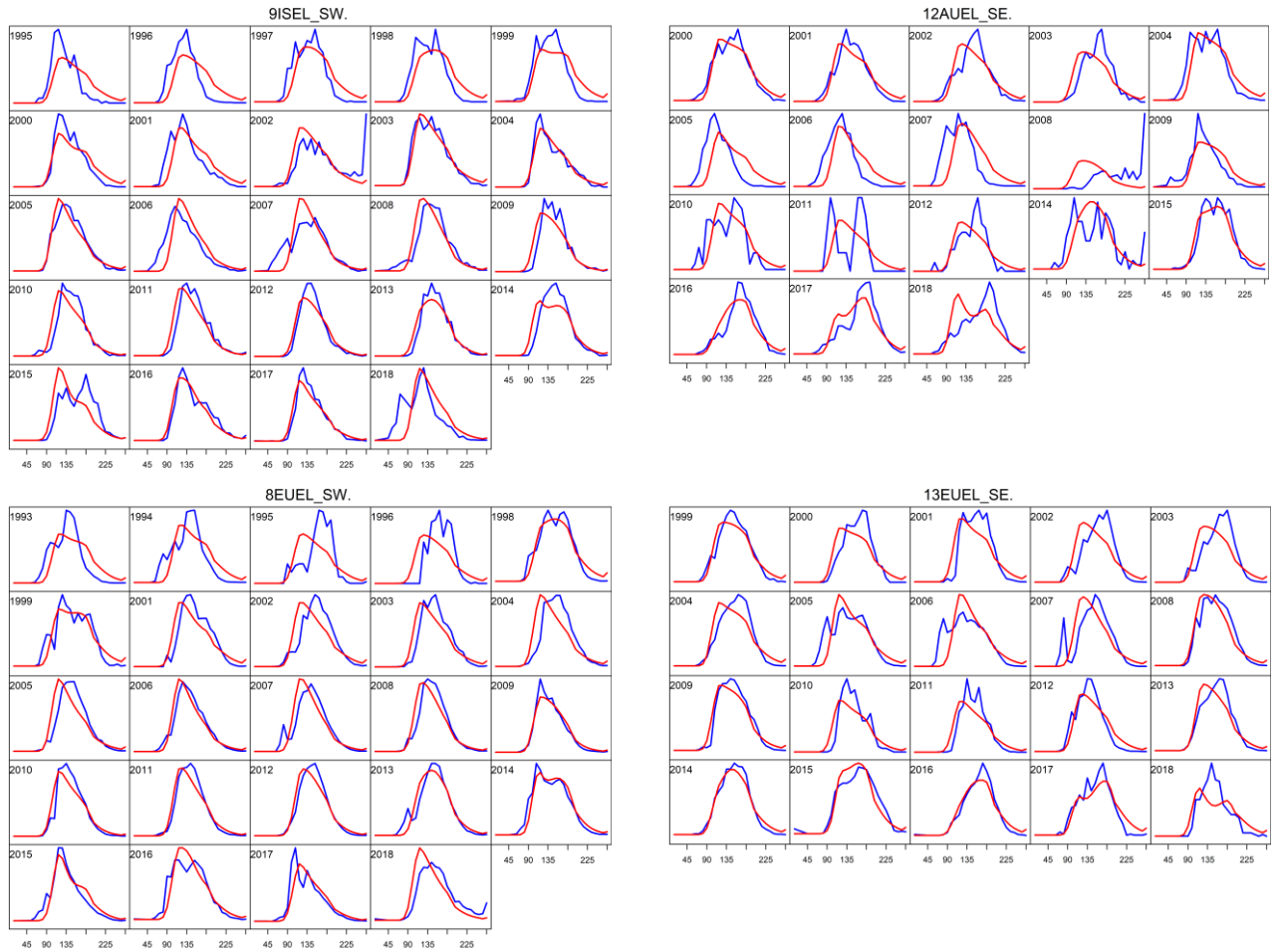
Figure A3. Observed (blue) and predicted (red) length compositions for the EUEL (SW and SE), AUEL, and ISEL fleets.
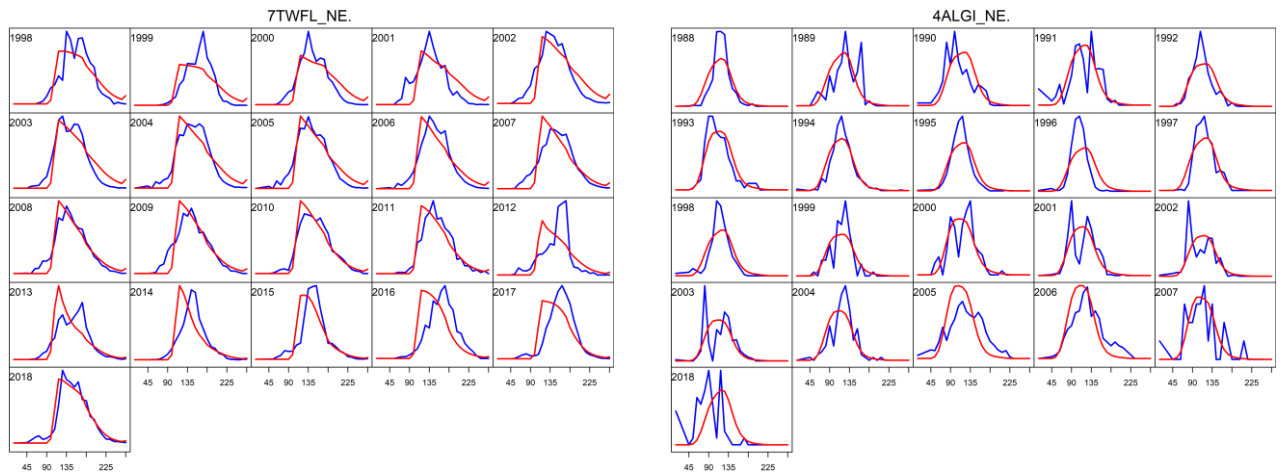

Figure A4. Observed (blue) and predicted (red) length compositions for the TWFL and ALGI fisheries.

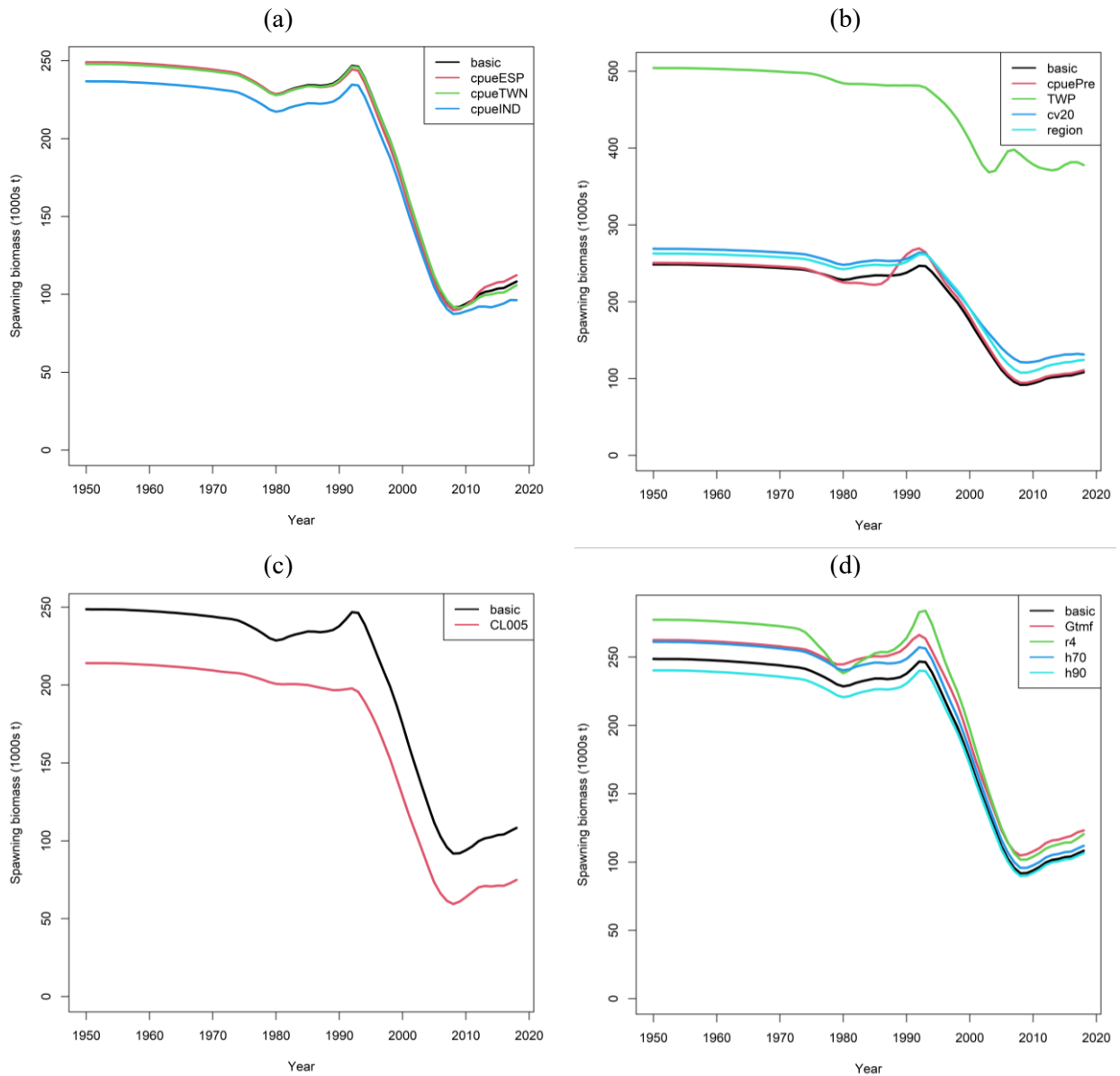## APPENDIX B: SELECTED RESULTS FROM THE SENSIVITY MODELS

Figure B1: A comparison of estimated spawning biomass from the basic model sensitivity models – (a) and (b), models related to CPUE options; (c), models related to sample sizes of length composition data; (d): models related on biological parameter assumptions. A description of the sensitivity models is given in Table 5.
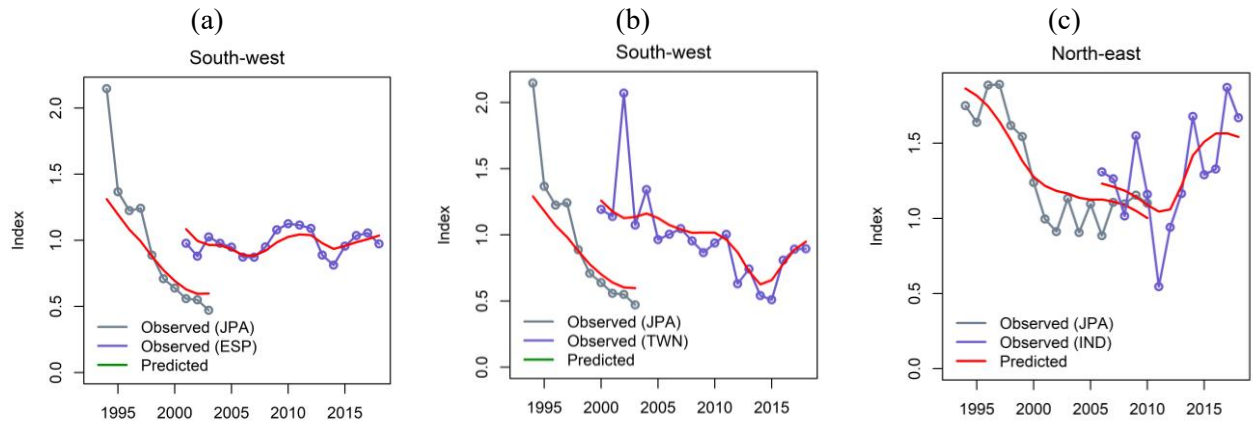
Figure B2: fits to selected CPUE indices from the three sensitivity models related to CPUE options, from model (a) *cpueESP*, (b) *cpueTWN*, and (c) *cpueIND*.
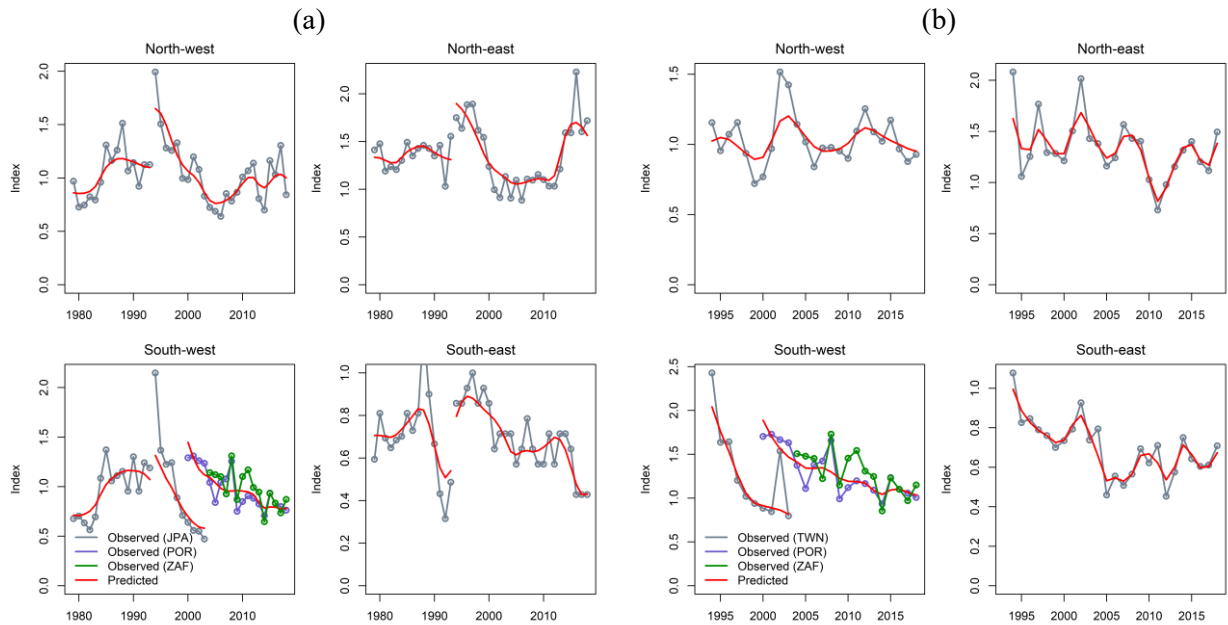

Figure B3: fits to CPUE indices from the two sensitivity models related to CPUE options, from model (a) *cpuePre*, (b) *TWP*.
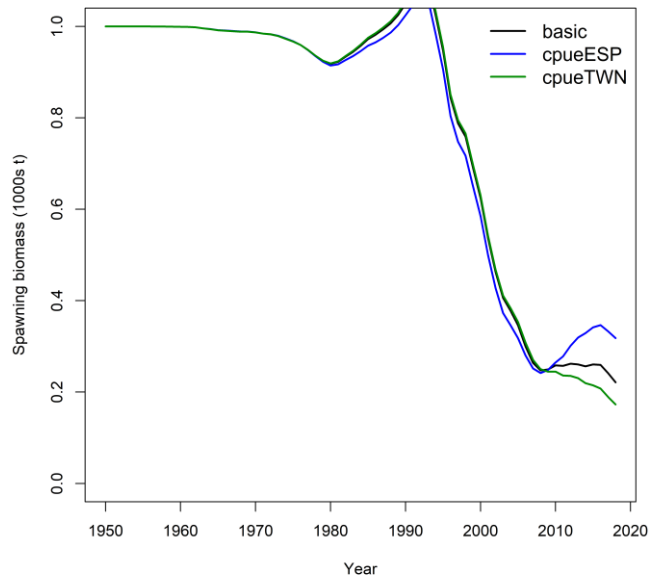
Figure B4: A comparison of estimated spawning biomass in the SW region from the basic model, and the sensitivity models *cpueESP* and *cpueTWN*.
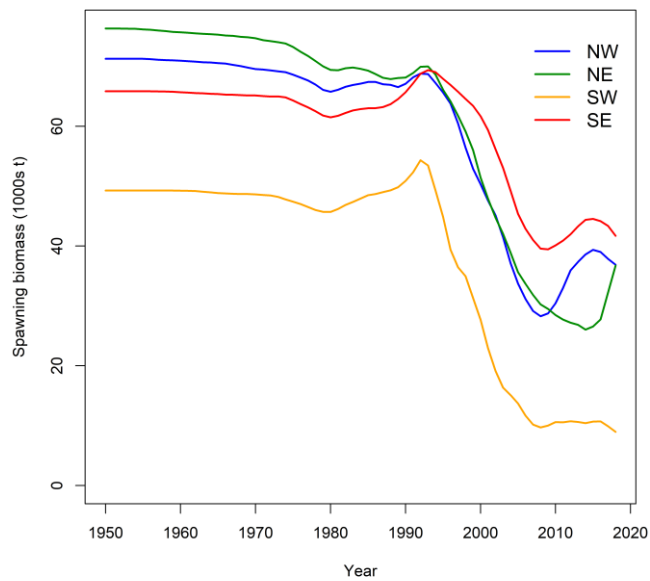

Figure B5: Estimated spawning biomass the individual model regions from the sensitivity model *region*.
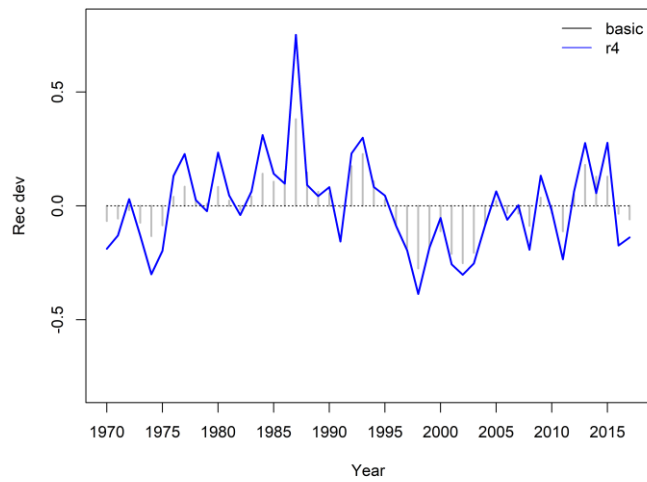
Figure B5: A comparison of estimated recruitment deviations from the sensitivity model *r4* to the basic model.

Table B1: Maximum Posterior Density (MPD) estimates of the main stock status indicators from the basic and sensitivity model options.

	SB_0	SB_{MSY}	SB_{MSY}/SB_0	SB_{2018}	SB_{2018}/SB_0	SB_{2018}/SB_{MSY}	F_{2018}/F_{MSY}	MSY
basic	248,650	58,607	0.24	108,315	0.44	1.85	0.58	32,951
cpueESP	249,066	58,379	0.23	112,303	0.45	1.92	0.56	33,046
cpueTWN	247,903	58,480	0.24	105,860	0.43	1.81	0.58	32,852
cpueIND	236,806	55,814	0.24	96,352	0.41	1.73	0.67	31,411
cpuePre	250,580	59,139	0.24	110,869	0.44	1.87	0.57	33,112
TWP	504,255	115,969	0.23	378,008	0.75	3.26	0.19	61,042
cv20	268,938	63,467	0.24	131,489	0.49	2.07	0.51	35,503
region	262,763	66,169	0.25	124,278	0.47	1.88	0.56	33,323
CL005	214,105	50,586	0.24	74,921	0.35	1.48	0.76	28,743
GtMf	262,497	62,035	0.24	123,160	0.47	1.99	0.53	34,987
r4	277,337	65,465	0.24	120,497	0.43	1.84	0.53	36,497
h70	214,105	50,586	0.24	74,921	0.35	1.48	0.76	28,743
h90	240,329	44,396	0.18	106,553	0.44	2.40	0.44	36,506